AFRL-PR-WP-TP-2006-242

OPTIMIZATION OF A LOW HEAT LOAD TURBINE INLET VANE

CAPT Jamie J. Johnson USAF, Dr. Paul I. King, Dr. John P. Clark, Dr. Michael J. Flanagan, and 2LT Ryan P. Lemaire USAF

JUNE 2006

Approved for public release; distribution is unlimited.

STINFO COPY

PROPULSION DIRECTORATE
AIR FORCE RESEARCH LABORATORY
AIR FORCE MATERIEL COMMAND
WRIGHT-PATTERSON AIR FORCE BASE, OH 45433-7251

REPORT DOCUMENTATION PAGE

Form Approved
OMB No. 0704-0188

1. REPORT DATE *(DD-MM-YY)*	2. REPORT TYPE	3. DATES COVERED *(From - To)*
June 2006	Conference paper postprint	10/01/2005-05/01/2006

4. TITLE AND SUBTITLE
OPTIMIZATION OF A LOW HEAT LOAD TURBINE INLET VANE

5a. CONTRACT NUMBER
In-House

5b. GRANT NUMBER

5c. PROGRAM ELEMENT NUMBER
62203F

6. AUTHOR(S)
CAPT Jamie J. Johnson USAF and Dr. Paul I. King (Air Force Inst. of Tech.)
Dr. John P. Clark, Dr. Michael J. Flanagan, and 2LT Ryan P. Lemaire USAF (Turbine Branch)

5d. PROJECT NUMBER
3066

5e. TASK NUMBER
06

5f. WORK UNIT NUMBER
303303W8

7. PERFORMING ORGANIZATION NAME(S) AND ADDRESS(ES)

Turbine Branch (PRTT), Turbine Engine Division
Propulsion Directorate
Air Force Materiel Command, Air Force Research Laboratory
Wright-Patterson AFB, OH 45433-7251

Air Force Institute of Technology

8. PERFORMING ORGANIZATION REPORT NUMBER
AFRL-PR-WP-TP-2006-242

9. SPONSORING/MONITORING AGENCY NAME(S) AND ADDRESS(ES)

Propulsion Directorate
Air Force Research Laboratory
Air Force Materiel Command
Wright-Patterson AFB, OH 45433-7251

10. SPONSORING/MONITORING AGENCY ACRONYM(S)
AFRL-PR-WP

11. SPONSORING/MONITORING AGENCY REPORT NUMBER(S)
AFRL-PR-WP-TP-2006-242

12. DISTRIBUTION/AVAILABILITY STATEMENT
Approved for public release; distribution is unlimited.

13. SUPPLEMENTARY NOTES
Published in 9th AIAA/ASME Joint Thermophysics and Heat Transfer Conference Proceedings, 5-8 June 2006, (AIAA-2006-3386). This material is declared a work of the U.S. Government and is not subject to copyright protection in the United States. Paper contains color. Best quality available.

14. ABSTRACT

Often there is a distinction between the design of turbomachinery airfoils for aerodynamic performance and durability. However, future aero-engine systems require ever increasing levels of turbine inlet temperature causing the durability and reliability of components to be an ever more important design concern. As a result, the need to incorporate heat transfer predictions into traditional aerodynamic design and optimization systems presents itself. Here, an effort to design an airfoil with both acceptable aerodynamics and minimized heat load is reported. First, a Reynolds-Averaged Navier-Stokes (RANS) flow solver was validated over different flow regimes as well as varying boundary conditions against extensive data available in literature. Next, a nominal turbine inlet vane was tested experimentally for unsteady heat load measurements in a linear cascade. The tests were performed in a reflected shock tunnel to validate the flow solver further at the current experimental conditions, and special attention was paid to leading edge and suction side heat-flux characteristics. The nominal airfoil geometry was then redesigned for minimum heat load by means of both design practice and two types of optimization algorithms. Finally, the new airfoil was tested experimentally and unsteady heat load trends were compared to design levels as well as the nominal vane counterpart.

Results indicate an appreciable reduction in heat load relative to the original vane. Thus, it is a credible proposition to design turbine airfoils for aero-performance and durability concurrently.

15. SUBJECT TERMS
Turbines, Heat Transfer, Vane, Durability, Reynolds Averaged Navier Stokes, Testing, Shock Tube, Unsteady

16. SECURITY CLASSIFICATION OF:			17. LIMITATION OF ABSTRACT:	18. NUMBER OF PAGES	19a. NAME OF RESPONSIBLE PERSON (Monitor)
a. REPORT	b. ABSTRACT	c. THIS PAGE			Dr. John P. Clark
Unclassified	Unclassified	Unclassified	SAR	30	19b. TELEPHONE NUMBER *(Include Area Code)* (937) 255-7152

Standard Form 298 (Rev. 8-98)
Prescribed by ANSI Std. Z39-18

AIAA-2006-3386
9th AIAA/ASME Joint Thermophysics and Heat Transfer Conference
San Francisco CA, 5-8 June 2006

Optimization of a Low Heat Load Turbine Inlet Vane

Captain Jamie J. Johnson, USAF* and Dr. Paul I. King.†
Air Force Institute of Technology, Wright-Patterson AFB, OH, 45433

Dr. John P. Clark‡, Dr. Michael J. Flanagan, and Second Lieutenant Ryan P. Lemaire, USAF
Air Force Research Laboratory, Wright-Patterson AFB, OH, 45433

Often there is a distinction between the design of turbomachinery airfoils for aerodynamic performance and durability. However, future aero-engine systems require ever increasing levels of turbine inlet temperature causing the durability and reliability of components to be an ever more important design concern. As a result, the need to incorporate heat transfer predictions into traditional aerodynamic design and optimization systems presents itself. Here, an effort to design an airfoil with both acceptable aerodynamics and minimized heat load is reported. First, a Reynolds-Averaged Navier-Stokes (RANS) flow solver was validated over different flow regimes as well as varying boundary conditions against extensive data available in literature. Next, a nominal turbine inlet vane was tested experimentally for unsteady heat load measurements in a linear cascade. The tests were performed in a reflected shock tunnel to validate the flow solver further at the current experimental conditions, and special attention was paid to leading edge and suction side heat-flux characteristics. The nominal airfoil geometry was then redesigned for minimum heat load by means of both design practice and two types of optimization algorithms. Finally, the new airfoil was tested experimentally and unsteady heat load trends were compared to design levels as well as the nominal vane counterpart. Results indicate an appreciable reduction in heat load relative to the original vane. Thus, it is a credible proposition to design turbine airfoils for aero-performance and durability concurrently.

Nomenclature

A/A*	=	Area ratio
AR	=	Aspect ratio
ex	=	Exit
in	=	Inlet
LE	=	Leading edge
M	=	Mach number
Nu	=	Nusselt number
P	=	Pressure
PS	=	Pressure surface
q"	=	Heat flux
Re	=	Reynolds number
s/s_x	=	Fractional surface distance
SS	=	Suction surface
St	=	Stanton number
T	=	Temperature
TE	=	Trailing edge
Tu	=	Freestream turbulence level
T_w/T_0	=	Gas-to-wall temperature ratio
u_τ	=	wall friction velocity
x/b_x	=	Fraction of axial distance
y+	=	Near-wall grid thickness Re
Δy	=	Near-wall grid element height
0	=	"Total" flow property
2	=	Exit condition
γ	=	Ratio of specific heats
θ	=	Momentum thickness
ν	=	Kinematic viscosity

* Student, Department of Aeronautics and Astronautics, 2950 Hobson Way, Member.
† Professor, Department of Aeronautics and Astronautics, 2950 Hobson Way, Senior Member.
‡ Senior Analyst, Turbine Branch, Propulsion Directorate, 1950 Fifth Street., Member

I. Introduction

Gas-turbine engine components are renowned for being designed for optimum aerodynamic performance at high pressure loading. However, turbine durability issues are becoming the focus of more turbine design programs as many component problems are ultimately traceable to a root cause involving heat transfer. Therefore, a lucid picture of the operating environment of turbine components should ideally precede a design for optimum aerodynamic performance. For example, supporting a turbine that has traded-off some aerodynamic qualities in favor of good thermal performance that yields a relatively long life is indisputably better than nurturing a turbine with optimum aerodynamic qualities and a shortened operating life due to a sub-par thermal design. Turbine components are subject to significant thermal stresses and high temperatures, so they are constantly susceptible to failure mechanisms such as hot corrosion, high-temperature oxidation, and thermal fatigue. Concepts including internal cooling passages, external film cooling, ceramic materials for structural members and thermal barrier coatings have all been implemented by industry in an effort to combat the unfavorable effects of excessive surface heat transfer. Yet these technologies have been most often used on vanes and blades with geometries designed primarily for aerodynamic performance rather than thermodynamic (i.e. aero-performance and durability). This effort, reported in more detail as a thesis[1], suggests the possibility of including heat transfer optimization of turbine airfoils along with traditional design for aero-performance. That is, the work suggests a unification of traditionally separate disciplines of turbine durability and aerodynamics.

A. Background

Historically, the design of turbine components specifically for reduced heat transfer has been done to a rather limited extent, perhaps due to the complexities of accurately modeling heat transfer in realistic turbine environments which often contain three-dimensional, unsteady, secondary, transonic, and turbulent flows. In addition, efforts focused on understanding turbine airfoil heat transfer have been commonly overshadowed by work done on the associated aerodynamics. Current standards in aircraft engines and research engines of the future demand affordable, efficient, light weight, and increasingly durable technologies, suggesting that further exploration of heat transfer issues relating to turbine component failure is in order. Turbine entry-temperatures are commonly well above the allowable metal temperatures of engine components. Since aircraft engines of the future demand ever-increasing performance levels, higher turbine inlet temperatures, and higher thrust-to-weight ratios, accurate turbine heat-transfer predictions are becoming more critical to gas-turbine design. Historically, increased performance characteristics relate to higher temperatures. Therefore, as turbine designers drive toward future gas-turbine engines, the primary goal is components that perform well under increasing heat loads and thus have superior durability with respect to previous engine designs.

This investigation focuses on the aerodynamic issues commonly associated with increased heat transfer including transition, free-stream turbulence, and pressure gradients all by means of manipulation of airfoil cross-section geometry. The logical place to begin this effort is in the hottest part of the turbine where extremely high turbine inlet temperatures exist, just downstream of the combustor, at what is commonly known as engine station four: the leading edge of the nozzle guide vane. The first step to ensuring turbine components do not fail under their harsh operating environment is the accurate prediction of the different causes and attributes of heat transfer on the turbine airfoil stator vane. Accurate local heat transfer predictions are required to improve vane service life and to reduce cooling requirements. A means to predict local heat transfer coefficients with accuracy has been a primary concern of researchers for years and a well-established design practice for predicting heat load can be a figure of merit for the design of future systems. Thus increased familiarity and prediction of the intricacies of the boundary layer on the airfoil surface is necessary. The transport properties of laminar and turbulent flows are very different, therefore proper prediction of overall heat transfer to turbine vanes and blades is critically dependent on the knowledge of the location and duration of the transition between these two regimes. As flow field property prediction methods have evolved to be a widely accepted science as will be discussed in the literature survey, the forthcoming techniques will offer an innovative and modern approach to designing and testing a 2-D turbine vane airfoil geometry explicitly for reduced surface heat transfer.

The problem of heat transfer starts in the properties of the air flow going through an engine. The extremely hot combustion products carry vast amounts of heat energy which are transferred through the surface of turbine components via the boundary layers created by the flow. Understanding boundary layer development is essential to understanding the surface heat transfer on turbine airfoils. Controlling the aspects of a boundary layer that contribute to heat transfer by manipulating the shape of an airfoil cross-section is the focus of this effort. While a thick laminar boundary layer may insulate a surface, the same thickness boundary layer that has experienced transition to a fully-turbulent flow regime will cause higher heat transfer due to a number of contributing factors. In

turbulent boundary layers, there is increased mixing (compared to laminar boundary layers where there is essentially no mixing) and thus more communication of thermal transport normal to a surface. There is also increased skin friction and shear stresses with turbulence, thus a higher magnitude of heat transfer. Generally, heat transfer and early transition has not been major concern on the pressure side turbine inlet guide vanes, where mostly favorable pressure gradients exist. While the gas temperatures on the pressure (concave) side of an airfoil are high, rarely does the flow on a vane in cascade become fully-turbulent, although the pressure side boundary layers can see small areas of turbulence followed by a relaminarization (Nicholson et al.[2]). On the other hand, since transition to turbulence on the suction side is much more prevalent due to the adverse pressure gradient experienced by the flow near the trailing edge of an airfoil, this will be an area of focus for this project. The challenge is to create an airfoil geometry that keeps the boundary layer laminar and smoothly accelerate the flow over the suction side thereby staving off transition to turbulence for as long as possible towards the trailing edge. However, there is a trade-off here. As a laminar boundary layer is accelerated (i.e. $dP/dx<<0$), the boundary layer thins causing higher surface temperature gradients and thus higher heat flux, but then it has not tripped into turbulence which causes mixing and increased skin friction. And while a thicker boundary layer insulates better, a thick turbulent boundary layer almost always causes higher heat transfer than a comparable laminar one. Achieving delayed transition reduces the amount of surface over which turbulence occurs, thus decreasing heat transfer. These methods will be discussed in more detail in the code validation and airfoil design optimization sections of this paper.

B. Previous Research

Much previous work has been conducted to examine the heat transfer trends exhibited in turbomachinery of jet engines and to compare those observations with the latest in predictive computational methods. However, very little has been does concerning direct optimization of airfoils for reduced heat transfer. Pertaining to fundamental heat flux measurement, Elrod[3] used flush-mounted Germanium thermocouples and a transient finite differencing scheme to obtain heat transfer rates on five midspan points (leading edge and ¼, ½ chord points on the PS and SS) on a vane in an eight-passage cascade mounted downstream of the same shock tube apparatus used in this work. Comparing reflected shock temperature ratio (T_5/T_1) to calculated heat transfer over a range of incident shock Mach numbers, he recognized increases from the leading edge (LE) to the ¼ chord point on the SS and attributed this to transition. A steady decrease in heat transfer from the LE to ½ chord point on the PS of the instrumented vane was also seen. Fillingim[4] took the above work a step further by increasing heat flux resolution and using three CALSPAN heat flux gauges on each side of a cascade vane and a thermocouple at the ¼ chord point on the SS. Increased heat transfer was also observed at the LE stagnation point and on the SS due to transition in which the start of transition appeared to move towards the leading edge for increasing test section inlet Mach numbers. Work pioneered by Dunn and Stoddard[5] resulted in some of the first significant experimental transient spatially resolved heat transfer data recorded in turbine-representative flows. Working with a state-of-the-art 176 degree stator vane annulus sector and demonstrating both a short-duration shock tunnel facility and Pyrex-platinum heat flux gauge technology, they discovered trends in the heat transfer in a turbine environment not seen before and identify heat transfer problem areas, such as towards the trailing edge of the vane suction side (SS) and near the leading edge on the vane pressure side (PS). Some of the first experimental evidence of SS transition to turbulence was concluded from these experiments. Dunn and Hause[6] later converted the shock-tunnel facility to accommodate a full annulus complete Garett TFE-731-2 turbine stage with stator and rotor to take heat flux and pressure data and compared results to Ref 5 and rig design estimates. The spatially resolved heat transfer results showed an increasing Stanton number (St) with increasing chord Reynolds number on the SS indicating the existence of boundary layer transition.

Concerning heat transfer experiments and respective code validation efforts, Wistanley et al.[7] compared the vane heat transfer work of Dunn[5] to predictions using flat plate correlations, a 2-D parabolic boundary layer code (STAN-5), and a 3-D viscous code (NANCY). He found that turbulent flat-plate correlations and post-transition boundary layer codes generally over-predict surface heat transfer, especially on the nozzle guide vane (NGV) SS, lending to the conclusion that more work was necessary to explore SS heat flux. Consigny and Richards[8] performed heat transfer measurements on a stationary rotor blade using the VKI light piston tunnel (LPT) for varying inlet Mach numbers, inlet Re, and inlet flow angles. The rotor was instrumented with 40 painted-on platinum thin films in a 6-blade cascade. They found that transition onset on both airfoil surfaces occurred earlier for increasing Re and turbulence level with higher Tu increasing the SS heat load. Comparing these runs at four different Tu to the 2-D two-equation kinetic energy dissipation model, or k-ϵ turbulence model, showed an under-prediction of SS heat transfer coefficient and a common lack of prediction of SS transition onset. Simoneau et al.[9] also noted this trend in their summary of flow prediction methods, in which this type of model at least gives good insight to 2-D type flows, such as at midspan.

Soon after, Dunn et al.[10, 11] used their own shock tunnel full stage heat transfer rig data from Ref 6 and data for three different T_0/T_w to compare to the STAN-5 code and an Air Force Research Laboratory (AFRL) Turbine Design System code (TDS). There was little effect on NGV St due to changes in T_0/T_w. The TDS code predicted NGV and the non-rotating rotor PS St reasonably well, in which there was early transition to turbulence on the NGV SS. With a rotor in motion, vane and blade boundary layers reportedly appeared turbulent. These turbulent behavior and early transition characteristics augment turbine component heat transfer, and are at the root of the investigation of this effort, especially for the optimization task. Still using the TFE 731-2 rig, Dunn[12] then took rotor blade heat transfer measurements at hub, midspan, and tip location of a blade downstream of an NGV that injected air out of the PS into the flow for two different cooling air-to-gas temperature ratios and compared the data to a flat-plate technique and the STAN-5 code. Results indicated another case of turbine component SS heat transfer unpredictability, as the flow at all three span locations transitioned at about 20% of the wetted suction surface and neither the laminar or turbulent flat plate correlation was effective, while the turbulent STAN-5 prediction only matched after 50% of the suction surface. PS heat transfer, however, was more predictable, even with the basic turbulent flat plate theory. Historically, cascade PS characteristics have been easily simulated, perhaps because in favorable pressure gradients the acceleration acts to stabilize the boundary layer and counteract the effect of free-stream turbulence as seen in the work by Blair[13].

Again using a shock tube to create short-duration turbine-representative inlet flows, Dunn[14] took on the Garrett low-aspect-ratio (AR = 1.5) turbine stage (LART) taking midspan NGV and blade heat transfer measurements and comparing them to flat-plate prediction methods. This low aspect ratio nature of the turbine component geometry is similar to that seen in the shock tube cascade experiments of this work. The vane Stanton number data unexpectedly well-exceeded the turbulent flat plate prediction, contrary to the trend seen in Ref 7, with transition occurring at 6% of the SS distance. The rotor data showed good prediction once again for the turbulent PS, while the SS data lay between the laminar and turbulent predictions, transitioning at about 30% of the surface distance. This augmented SS St compared to prediction, possibly due to unsteady boundary layer heat transfer phenomena, leaves much to be explored. This trend is also seen when Rae et al.[15] compares two inviscid NASA codes named MERIDL and TSONIC and the STAN-5 code to two different rig heat transfer data sets, both recorded by Dunn using the LART and the TFE rigs. Comparison of the LART data to the NASA codes for transitional and turbulent values of Re_θ shows midspan SS St magnitudes exceeding the predictions by a ratio of 2:1. However, the PS rotor comparison fared well. Comparisons of the LART data to the k-ϵ model were done at two levels of Tu (5 and 10%). Even still, the models did not come close to predicting the vane SS and PS data which was again twice the magnitude of the prediction of the k-ϵ model. Also, in line with the history of the comparisons outlined above, the rotor data was relatively well matched with prediction, perhaps because the rotor is insulated from any eccentric inlet flow characteristics seen by the NGV. More recently, Haldemann et al.[16] conducted heat transfer measurements at 20, 50, and 80% span using the shock-tunnel of Dunn on an inlet vane and compared the data to a KEP boundary layer prediction technique of Suo and Lounsbury in which St at 50% and 80% span was mostly under-predicted, except at the LE. The predictions were quoted as being "not particularly good at any of the spanwise locations [of the vane]".

Concerning turbulence effects on heat transfer, the works of Blair et al. and Galassi et al. both produced profound results towards this end. Blair et al.[17] studied midspan heat transfer for a turbine inlet stator, rotor, and second stator using the UTRC large, low-speed steady flow stage-and-a-half turbine at 0.5% and 10% Tu. The first vane row showed a dramatic effect of inlet Tu on increased heat transfer, with transition occurring very early on the SS, while the rotor and second stator saw little heat transfer magnitude dependence on Tu, which also lends credence to the postulate that flow regulated by the vane diminishes the probability of downstream components seeing wildly 3-D unsteady effects and resultant heat transfer augmentation. In comparison to a finite-difference boundary layer code for laminar and turbulent predictions, both the first and second stator Stanton number were greatly under-predicted by the turbulent model on both the vanes' PS and SS surfaces. Galassi et al.[18] used a 4-blade cascade and jet-grid with three injection orientations and two upstream locations to examine intensity and length scale effects on St. They compared measured St in grid-out runs with a laminar equation for St from Kays and Crawford[19], while the grid-in runs were compared to the method of Ambrok for turbulent flow St. Data correlated well with the laminar and turbulent predictions. With the jet-grid installed, SS transition onset moved from 70% of the surface distance for no grid to 10% for the near-station grid and 20% for the far-station grid. A proportional relationship between Tu and St was witnessed along with an inverse relationship for length scale size and Nusselt number (Nu). This was yet another case of augmented SS heat transfer due to early transition.

Lastly, Giel et al.[20] also performed studies measuring heat flux using liquid crystals for a stationary 12-blade cascade for two inlet Re, two M_2, and turbulence grid in (Tu = 7%) and out (Tu = 0.25%) cases. Here, high Re and high Tu (grid in) both contributed to early SS transition, almost near the LE stagnation point. This complies with the detailed boundary layer measurements of Radomsky et al.[21], which stated that for very high (i.e. combustor

level) Tu, the integral parameters on the SS moved upstream compared to low Tu levels, thus effecting skin friction and heat transfer. Comparing the experimental results of Giel to the 3-D Navier-Stokes code (RVC3-D), transition onset was fairly predicted but the following was determined: LE heat transfer was under-predicted for low Tu and Re cases, PS values were under-predicted for all high Tu cases, and for all high Re cases (regardless of Tu) the SS heat transfer was under-predicted over the whole surface distance. Boyle et al.[22] performed perhaps the definitive prediction method breakdown comparing four models for predicting Stanton number due to varied Tu with sets of vane data compiled by Ames et al., Radomsky and Thole, and Arts[23] from a wide range of flow conditions. While other models exhibited interesting trends, the prediction results of the Abu-Ghannam and Shaw (AGS) transition length model is of primary interest as it was a critical part of the flow-solver code used in this effort. Boyle concluded that in general the AGS model predicted vane PS heat transfer well, is preferred for higher Re flows, uses a conservative length model with transition duration being predicted as often too long, and on some occasions under-predicted SS heat transfer. The trends in all of these cases indicated early transition from higher Tu and inlet Re and an under-prediction of SS heat transfer when compared to various prediction codes.

Again, very little information exists in the literature on the optimization of turbine components specifically for low heat transfer. However, there are a large number of researchers who have used optimization techniques in similar areas of study. Nicholson et al.[2] conducted some of the original studies of this nature comparing pressure profiles and heat transfer on the pressure and suction surfaces of two different rotor blades of different stagger angles in a linear 2-D cascade row at the end of an isentropic light piston tunnel which ran at varying conditions. Using vanes with pressure side optimized geometries, they found that SS transition was very common and moved forward with increasing Re and that increased Tu causes augmented mean heat transfer rates. Similar trends have been seen in the predictions of the current work. The study effectively built on the prospect of minimizing heat transfer via boundary layer control methods and it was concluded that aerodynamic efficiency is not compromised by a heat-transfer-optimized design.

Algorithms have been used quite extensively since the mid-1990s to solve optimization problems using objective functions. More specifically, genetic algorithms have been successfully employed in the past by Durbin et al.[24], Obayashi and Tsukhara[25], and Anguita et al.[26] to define optimally contoured infinite cascade endwalls, maximize the lift coefficient of a wing airfoil, and design a turbine blade with low loss and high loading, respectively. These and many other works since then support the use of GAs, which will be utilized in the re-design and optimization of the nominal turbine vane in this work.

The preceding case studies present an outstanding case for the need to further understand turbine nozzle guide vane leading edge and suction side heat transfer characteristics and through modern optimization algorithms create a high thermal performance vane with acceptably lowered heat load qualities, which can be properly validated by both modern predictive and experimental methods.

C. Current Study

The primary goal of this work is to attempt to design a 2-D turbine vane airfoil that has a reduced heat transfer load at midspan (half-way between the hub and tip on the vane) solely due to its geometry. The primary hypothesis of this problem is that through design, a vane airfoil geometry can be generated that exhibits reduced heat transfer. In order to efficiently attack this problem, tools will be necessary to design the airfoil and ensure that the theoretical heat transfer is accurate by validating existing computational codes. So, a nominal airfoil with extensive known experimental data concerning its heat transfer and pressure loadings will be selected for code validation, and a new airfoil will be designed for reduced heat transfer and compared to the nominal airfoil through suitable experimentation. More specifically, the goals are: 1) To validate a RANS flow-solver by comparison of the experimental data from the nominal airfoil to the results of the code for the same boundary conditions, 2) To use a novel turbomachinery design system (TDAAS)[27] used by the Air Force Research Laboratory (AFRL) in concert with the validated code to optimize the nominal 2-D vane airfoil and transform it to a geometry with reduced theoretical heat transfer while having good aerodynamic qualities, and 3) To compare two turbine stator vanes and observe a lower heat load in the optimized vane by means of linear cascade experiments. For the latter goal, turbine-like flow conditions are to be created in a shock tube facility used in the past for Air Force Institute of Technology (AFIT) and AFRL experimental purposes. It is anticipated that the following report will be a step towards a modern solution to an old and pervasive problem in the turbomachinery design industry and contribute to a more accurate prediction of heat transfer on turbine stators and increased confidence in numerical heat transfer prediction and optimization methods for reduced heat load.

II. Code Validation and Airfoil Optimization Methodology

A. CFD Code Validation

To begin this effort, a code needed to be validated and an airfoil to validate the code had to be chosen. The code used in this effort, currently used by NASA Marshall, is a quasi-three dimensional viscous fluid dynamics analysis tool for axial flow turbomachinery vane and blade rows named WILDCAT by Dorney[28]. The studies here will be restricted primarily to 2-D as it only deals with an airfoil geometry at midspan. The WILDCAT code has the ability to predict steady or unsteady flow fields for single or multiple blade rows and generate grids for the calculations using another code called WILDGRD. For simplicity, the code will be referred to solely as WILDCAT. The analysis is performed mathematically using the numerical solution of the Navier-Stokes equations. The numerical technique used in the solution is a time marching, implicit, upwind finite-difference scheme with a zonal, mixed grid topology. It is second order accurate in time and third order in space. The details of this Navier-Stokes numerical scheme can be reviewed in Ref 29. The code solves the flowfield on two overset grids, an O and an H grid, which are used to make the sequential temporal numerical calculations through the vane passage.

Next, an airfoil with an extensive pressure loading and heat transfer database at a wide range of conditions was selected for validation. This baseline airfoil, which will be referred to from here on as the VKI vane, is a highly loaded transonic turbine nozzle guide vane that experienced extensive aero-thermal cascade testing in the von Karman Institute (VKI) short duration Isentropic Light Piston Compression Tube facility. The measurements taken on the vane were compiled and documented by Arts et al.[23] in which tests were performed for several combinations of freestream flow parameters, primarily Reynolds number (Re), turbulence intensity (Tu), and Mach number (M), in order to assess aerodynamic performance and convective heat transfer characteristics. The VKI vane was a logical choice since the original intent of this experimental database was to use the data for validation of both inviscid and viscous calculation methods. The VKI test program consisted of 7 blade velocity distribution (pressure loading) runs and 21 convective heat transfer runs with varied freestream conditions according to the following ranges: $T_0 = 420$ K, $M_2 = 0.7$ to 1.1, $Re_2 = 5x10^5$ to $2x10^6$ and Tu = 1.0 to 6.0%. Figure 1 shows the VKI vane geometry plotted on fractional axial chord coordinates with the position of the flow passage throat indicated. The grid employed a near-wall grid thickness Reynolds number, $y+ = (\Delta y\ u_\tau)/\nu \leq 1.0$ all around the airfoil surface. Commonly, $y+ < 1$ is acceptable for two-equation turbulence models and $y+ < 3.0$ is acceptable for the Baldwin-Lomax turbulence model[30] which is used in this case by the WILDCAT code. The size in I-J coordinates of the O grid is I = 121 by J = 23 while the size of the H grid is I = 60 by J = 30. The O grid has a near-wall grid element height $\Delta y = 1.27$ μm.

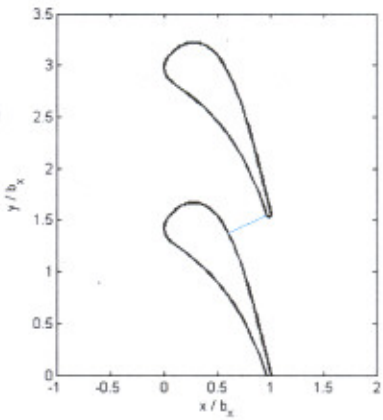

Figure 1 – VKI vane cross-section shape.

The WILDCAT code was embedded in an easy-to-use MATLAB turbine design and analysis system (TDAAS) used by turbine component designers at AFRL and created by Clark[27]. The design system allowed the user to have a graphical user interface (GUI) for efficient operation of the grid generator and flow solver code using simple menus to input information. Using the WILDCAT code in the design system, once an airfoil coordinate geometry was read into the code, a grid of the desired type was generated, all the necessary flow condition parameters and desired number of iterations were entered, and the code was executed. The code could ultimately compute the resulting flow field properties as they apply to heat transfer, pressures, Mach numbers, boundary layer characteristics, and more. The WILDCAT code was used to input the appropriate unique flow conditions for each run and simulate all 7 of the pressure loading and all 21 of the convective heat transfer trials performed experimentally by VKI and compare the code output with the actual data produced by the VKI vane in their cascade. For the most part, using the heat transfer grid, all pressure loading and heat transfer predictions were run for at least 10,000 iterations which gave a generous amount of convergence. Key variable boundary conditions that were entered before each run included the following: the isentropic exit Mach number, total temperature upstream of the vane, the total pressure upstream of the vane, the freestream turbulence level, and the vane wall boundary condition. As VKI provided the wall temperature for each of the heat transfer runs, only the Dirichlet condition was used for validation purposes. The code also solved the laminar and turbulent forms of the Navier-Stokes equations. WILDCAT assumed transition onset as defined by a number of models. For validation purposes only the Abu-Ghannam and Shaw (AGS) transition model[31] was chosen to be studied against the VKI data. These WILDCAT runs were repeated until

a wide enough set of flow conditions were covered to deem the code validation complete for the experimental data of the VKI vane and the relative WILDCAT results.

B. Airfoil Re-design and Optimization

Optimization of the VKI vane for reduced heat transfer was a rigorous, iterative design and computation process. The MATLAB design and analysis system for turbine airfoils recently implemented at the Air Force Research Laboratory by Clark[27] was critical to the optimization task. Complete details of the system are not releasable in open forum at present, but the basic methodology as it applies to the current study is given here. The system employs an industry-standard airfoil shape-generation algorithm developed by Huber[32] to define turbine blade and vane shapes. The grid generator and flow solver of Dorney and Davis[29] are used to determine the aerothermodynamic behavior of the design shapes. The shape and grid generators and the flow solver are then combined with GUI-based flow-field-interrogation and design-optimization techniques to allow a designer to realize new and/or improved airfoils in short order. The optimization can proceed via either gradient based (sequential quadratic programming) or genetic algorithms (GA), and a wide range of objective functions are specifiable by the user. For example it can be used to reduce loss, manipulate the pressure loading characteristics of an airfoil, or minimize heat flux at specified areas for an airfoil surface, as is the focus of this study. Among other advantages, this design system allows reverse-engineering in which the user can specify the desired flow characteristics or performance goals and generate a new airfoil shape based on these.

At first, the main idea of this work was to reduce the overall heat load on the optimized vane relative to the baseline VKI vane. This objective may be ambiguous since the optimized airfoil may have a lower integrated heat load over both the pressure and suction surfaces compared to the VKI vane, but have one or more hot spots that would cause failure of surface material integrity in an actual engine test. Ideally, the new airfoil must also perform well aerodynamically (low loss, high loading) and have reduced surface heat transfer characteristics when tested either computationally or experimentally. Also, the re-design and optimization process is a balance of both art and science. Both good judgment (art) and extensive parameter analysis (science) went into the formation of the optimized airfoil. The two main objectives of the optimization were to (1) reduce leading edge (LE) heat transfer and (2) drive back transition on the suction side as far possible towards the trailing edge (TE).

Knowing that heat flux is heat transfer per unit area, if the area is increased, then the heat flux must decrease. Also, the larger the radius of curvature is the lower the level of heat flux[19]. To achieve the goal of reduced LE heat transfer, it was postulated that increasing the leading edge diameter (LED) parameter of the airfoil would help provide a solution. A great amount of attention was given to this objective in hand-iterations, or the art of the optimization process. Of course, changing the LED meant other parameters would change as well in order to keep pressure loading and SS heat transfer acceptable. These hand-iterations, or any other automated optimization iterations performed, were saved in a design log file which could be reviewed at any time. The user could scroll through all optimization iterations completed showing the respective airfoil shape, fractional surface distance pressure loading, and heat transfer plots. This invaluable tool gave good indication as to whether the optimization was headed in the right direction as it pertains to the design objectives. This guaranteed efficient design progression as the current best airfoil could be accepted and run in WILDCAT with slight changes in parameters and then immediately compared to the previous design using the design log history. Concerning the second objective, a *Drive to Target Loading* function[27] allowed the designer to reverse-engineer airfoils. During the re-design of the VKI vane it was determined from the AGS transition model[31] that derived the start of transition from turbulence level and a pressure-gradient parameter, and from design practice with the interactive GUI, that driving the minimum SS $P/P_{t,in}$ back towards the TE of the airfoil generally resulted in delayed transition. This assumes the minimum was arrived at with as little oscillation in pressure gradient as possible. The airfoil pressure loading results from a WILDCAT run could be examined and the *Drive to Target Loading* function allowed the actual graph of the SS pressure ratio to be manipulated by the user with the mouse pointer and submitted to the sequential quadratic programming (SQP) optimizer algorithm. Then, the airfoil shape would be changed in order to get as close to the desired loading as possible—hence the reverse engineering aspect of the design system. This method was successful in arriving at the delayed theoretical transition characteristics of the final optimized vane selected.

Another tool used in the airfoil optimization process was a genetic algorithm, or GA. GAs, have been used frequently in recent aerodynamic design practice for optimization purposes[25, 26]. They can readily locate an optimal point in a problem space of theoretically infinite dimensions. In other words, much like the SQP algorithm, the turbine designer can vary several parameters and input desired ranges of these parameters related to the quantity optimized. Genetic algorithms are a process for function optimization that mimics the genetic reproduction process experienced by biological organisms. The GA uses fitness functions prescribed by the user to determine the best option available. Fitness functions were used that best represented the priority of the airfoil parameters that were being optimized, such as heat transfer, which was a result of multiple other parameters. Careful implementation of a fitness function, which is subjective to the designer, will result in a significantly improved airfoil in minimum time by using the process of natural selection to improve the set of parameters, or genes, that describe the airfoil. The GA is not perfect, however, as it is susceptible to mutations and elitism, which makes the structure of the fitness function critical to the success of the GA. Here the nature of the fitness functions, or objective functions, stayed close to the two main goals for the optimization for reducing LE heat load, and manipulating the SS curves to delay transition towards the vane TE. A population size of 40 was chosen and the number of generations for this case was 38. The initial code structure, variables used, and methodology which laid the groundwork for commanding the desired objectives in the fitness functions relating to reduced heat transfer design was accomplished by J. Dagg. The approximate average computation time for the genetic algorithm operations alone to find a heat transfer optimized airfoil was approximately 5 days. Figure 2 is a flow chart with the basic steps of the algorithm and screen shots of the MATLAB GA optimization suite windows that were used to execute the runs. Constraints of the optimization of the VKI vane included keeping the axial chord constant (at 0.8575 in) for simplicity and interchangeability when it came time to test each vane cascade using the shock tube and using a single set of flow conditions (VKI MUR237 cascade heat transfer experimental run). These flow conditions were chosen for their applicability to a realistic modern turbine inlet environment and because they would match the conditions for a turbulence grid-installed shock tube run when it came time to record experimental heat transfer for both vanes.

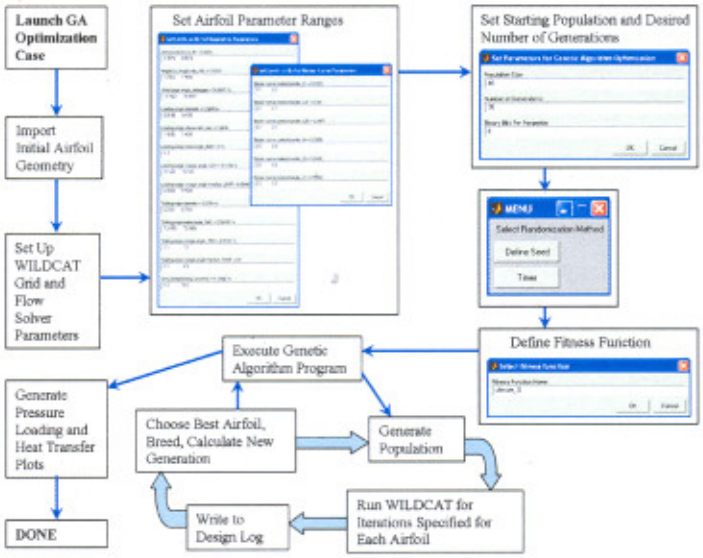

Figure 2 – Genetic Algorithm Process Methodology

In summary, the VKI airfoil was transformed and redesigned to the desired lowered heat transfer specifications using following the steps: 1) The airfoil was run through numerous automated SQP optimization iterations to reduce overall heat load, 2) Knowing the objective of step 1 was too ambiguous and unsatisfied with the results in that step, the two main objectives stated above were enforced, 3) The *Drive to Target Loading* function with SQP optimization was used to attempt to delay transition, 4) Hand-iterations and good design judgment were used to aid in reducing LE heat load by examining airfoils with large LEDs which supplied a favorable starting position for the GA process, and 5) The best airfoil obtained from the process above was entered into a 40 object by 38 generation GA which further explored the problem space reiterating the objectives and the best GA airfoil calculated was selected. As a result, suitable airfoil geometry had been created that met the two main objectives pertaining to reduced surface heat load. Hereafter, the new geometry will be referred to as the low-heat-load vane, or LHL. Once a solution was found, the two airfoils could then be compared in a real turbine-representative flow environment.

III. Experimental Setup

Many different facilities have been used in the past to perform turbine related heat transfer studies. They essentially fall into two main categories, long run-time (i.e. steady state) facilities and those that have short run durations. Notable long run-time facilities include those used by Blair[17], Graziani[33] and York[34] which tend to be more common in industry. Short run-time facilities of distinction include the shock tunnel facility used extensively

by Dunn et al. and the isentropic light piston tunnel (ILPT) employed by Nicholson et al.[35] The apparatus used here falls into the latter category, along the lines of the facilities used by Dunn et al.[5], as short-duration methods use much less power, are less expensive to operate, and are regularly much more convenient and repeatable than long run-time flow facilities. In addition, as seen by the above works, short run-time facilities have long been established as a validated technique for performing aerodynamic and heat transfer measurements.

For the experiment at hand, a rectangular cross-section, low shock pressure ratio shock tube used in past AFIT theses experiments by Frye[36], Gochenaur[37] and Fillingim[4] was used to model the high temperature, high pressure environment of a turbine inlet in order to measure heat transfer on the nominal and optimized vanes in a turbine-representative environment. The shock tube, currently in use by AFRL, consists of a high pressure driver section and a relatively low pressure driven section separated by a diaphragm. The driver section can be pumped up to a desired pressure while the driven side can be evacuated to a desired pressure to increase the magnitude of shock pressure ratio. In the current experiment, only the driver side pressure was increased and the driven side was kept at atmospheric pressure. Using well established transient test techniques, the shock tube can be used to obtain spatially resolved heat transfer rates on different gas turbine components. The shock tube is a total of 16 ft in length with a 4 ft long (1.22 m) driver section and a 12 ft (3.66 m) driven section and a uniform rectangular internal cross section 4 in (10.15 cm) by 8 in (20.32 cm). The shock tube itself is described in greater detail by Frye[36]. A 120 psi compressor air supply system was used to increase and control the driver side pressure. The driver section lies on a 2-axis mobile platform for ease of repeatability of experimental runs in replacing diaphragms and removing used diaphragm fragments. Once a proper diaphragm is installed, the driver and driven sections are held together with a hydraulic clamp built on to the driven section and operated using a hand-pump. Mylar sheets of varying thickness are available for use in the shock tube as diaphragms to separate the two sections. For the purposes of this effort, the diaphragms used were 0.007 in thick and installed with thin rubber gaskets on both sides between the clamped sections to help prevent air leakage. The diaphragm was ruptured and the shock initiated using a non-intrusive hand-trigger-operated pneumatic spike built into the center of the driver section. The shock tube was connected to the vane cascade test section at the end of the driven section.

The test section used in the current experiment made it possible to take valuable data concerning the heat transfer at midpsan for both the VKI and LHL vanes. The linear cascade consisted of 7 airfoils mounted with a 0 deg inlet angle, in which only the 4th airfoil for each of the vane geometries were instrumented for heat flux assessment. The vanes were separated by a pitch of 1.33 in creating six passages between vanes to provide for good flow periodicity. This resulted in a solidity of 0.64 and pitch-to-chord ratio of about 1.56. The original nozzle guide vane tested by VKI had an axial chord of 1.645 in. The vanes tested in the shock tube cascade are approximately half scale (52%), having an axial chord of 0.8575 in, which results in a relatively low aspect ratio of 1.166. The chord value was used in the numerical portion of this work for both the VKI and LHL vane and kept constant as a main control to simplify the optimization of the vane and reduce complexities due to the necessity of different turbine stage axial dimensions caused by larger or smaller axial chord lengths. High freestream turbulence conditions were simulated with the insertion of a turbulence grid upstream of the test section designed for 6% Tu. The grid was removed for low Tu experimental conditions. It should be noted that while the pressure and temperature entering the cascade test section provide realistic non-dimensional flow parameters, the flow in the experiment is atmospheric air and not combustion products from a combustor as in the real environment of a turbine engine inlet.

The cascade vanes were chosen to be comparable with typical turbine engine flow conditions. Table 1 shows that both vanes being tested experimentally have exit Mach numbers consistent with modern high reaction turbines. In addition, their pitch-to-chord ratios and Zweifel coefficients are larger than state-of-the-art military turbines (e.g., the F119 and F120). So, since the vanes happen to show evidence of healthy aerodynamic qualities they are a suitable step in the direction of the HIT turbine rig, which is itself a representative turbine for future long-range strike aircraft.

Table 1 – Comparison of VKI and LHL vane details with modern nozzle guide vanes.

Vane Details	F119	F120	HIT TR	VKI	LHL
Exit Mach Number	0.82	0.67	0.89	0.80	0.80
Pitch / Axial Chord	1.39	1.46	1.91	1.56	1.56
Zweifel Coefficient	0.73	0.74	0.85	0.79	0.77
Turning (degrees)	75	74	78	75	75

The framework for the test section is the same used by Gochenaur[37] and Fillingim[4] in their work. Seven identical, smooth ABS (Acrylonitrile Butadiene Styrene) plastic vanes fabricated in the AFIT 3-D printer plated with a very thin layer of copper 15 mils thick made up the linear cascade situated between two ¾ in clear plexiglass walls which were screwed together by the metal framework on the outside. The copper layer was added to make the vane surfaces smoother than if they were just the rough plastic from the 3-D printer. It was decided that since the layer of

copper was so thin relative to the thickness of the vanes, that the plastic vane thicknesses did not have to be reduced to accommodate the copper thickness. The inlet and outlet areas were 2 and 8 in^2, respectively, thus the throat of the test section is at its exit. The cascade lies 1 inch downstream of the test section inlet. Both sets of vanes had the same value of flow turning, about 75°, just as they did for their CFD analyses. The inlet Mach number upstream of the cascade row can be estimated from the known test section area ratio, $A/A^* = 4$. From isentropic relation tables for air (assuming $\gamma = 1.4$) this critical area ratio corresponds to an inlet Mach number, M, of about 0.15 and an inlet static to total pressure ratio, P_{in}/P_0, of about 0.98. From this P_0 can be found and knowing that the exit static to total pressure ratio is found by $P_{ex}/P_0 = P_{ex}/P_{in} * P_{in}/P_0$, the exit isentropic Mach numbers are found to be between about 0.80 and 0.85 for most runs. This value is comparable with the vane exit Mach numbers seen in Table 1 by designers of a future research turbine (high-impact turbine rig, or HIT TR) and by Gochenaur[37], Fillingim[4], Dunn[11], and Arts[23]. The test section plexiglass walls held the vanes in place by compression using metal pins, three per vane, and these lie in a pattern such that both the VKI or LHL vanes were interchangeable for testing at any time. The cascade vanes each had a span of 1 in. Since this is a relatively short vane span, there is good reason to believe secondary flow effects could hinder quality heat flux data at midspan. A detailed analysis of the 3-D vane flow-field in the test section using CFD tools and recent empirical prediction techniques from open literature show that the 1 inch flow width is rather worthy for making midspan measurements here. The examination revealed that horseshoe vortices generated due to end wall secondary flow only propagates to 15% span on each end of the vane at the trailing edge, suggesting it is safe to monitor flow properties such as heat flux at 50% span.

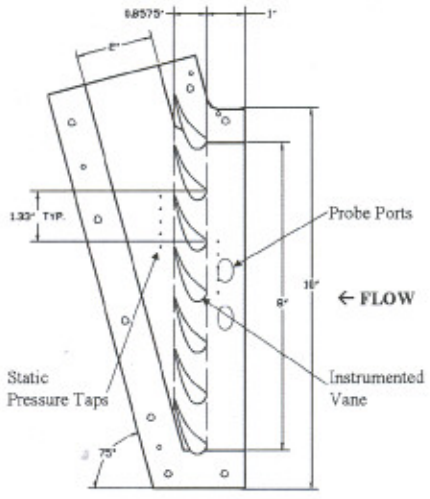

Figure 3 – Diagram of shock tube linear cascade test section (shown with VKI vanes installed).

Figure 3 is a schematic of the shock tube linear cascade test section and its main features with the air flow going from right to left. The static pressure tap arrays upstream and downstream of the vane row in the plexiglass end wall were essential in calculating Mach numbers for each run. The two other instrumentation ports positioned on the opposite plexiglass end wall were used for probes to record total temperature (T_t) and total pressure (P_t). These same ports would later be used to measure Tu and length scales using a hot-wire anemometer probe to test the grid and make comparisons with the grid design Tu. No dump tank was attached to the end of the test section as in previous works using the shock tube since there was no need to add one, and the flow through the shock tube exited to atmosphere.

Modern high-density thin film heat flux gauges fabricated and designed at AFRL[38] were used to obtain heat transfer data at the midspan of each vane in order to compare the VKI to the LHL vane in the turbine-representative shock tube test section environment. The gauges designed specifically for this experiment are fundamentally similar to those used by Dunn[14] and others in the past in that voltage changes are measured across a thin film resistance under constant current. However, the high density array gauges used here follow the design methods of Anthony[39] and that they have many advantages over older technology gauges. These flexible films are virtually non-intrusive to the flow lying flush on the curved surface of the vanes. The gauges are composed of a thin flexible Kapton insulating substrate layer 50 microns thick with known thermal properties underneath a thin layer of conducting platinum metal 500 Angstroms thick sputtered on top. They were carefully adhered to the VKI and LHL vanes to be positioned in the middle of their respective cascades using an adhesive 50 microns thick. The platinum thin films with substrate are designed very thin so they may be applied to any surface to make measurements, thus the instrumented vane in the middle of the test section vane row was not reduced or undercut to accommodate the small thickness of the films. Further details on the fundamental operation of the films are given in Ref 1.

The VKI and LHL vanes had a total of 27 and 28 midspan thin film gauges, respectively, since the LHL vane had a slightly larger surface distance. The VKI vane had 10 gauges on the PS and 17 on the SS, while the LHL vane had 10 gauges on the PS and 18 on the SS. The sizes of each gauge are consistent with good design practice meeting the minimum 10:1 length-to-width ratio recommended for good data collection[39]. Finally, to properly investigate the heat transfer around the airfoil, as the focus areas for this study as described before were reduced LE heat load and delayed transition, the gauge densities were increased (and the gauge sizes were decreased to the minimum possible size) near the leading edge and past approximately 50% of the suction surface for each vane. This provided increased data resolution around the surface in the areas of interest. There were two different gauge

sizes on the thin films, in which the small gauges measured 0.2 mm by 2.0 mm while large gauges were 0.4 mm by 4.0 mm. As a result, large gauges had 4 times the area of the small gauges, and as a fundamental design requirement, the aspect ratio for all gauges were subsequently kept constant. All gauges were spaced 0.2 mm apart. Figure 4 shows the fully instrumented VKI vane.

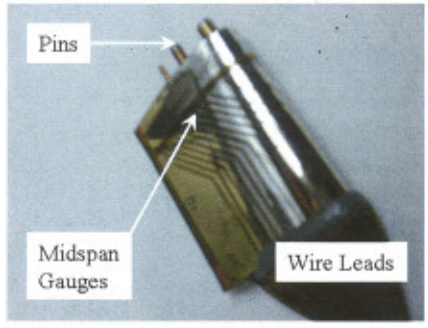

Figure 4 – Thin film heat flux gauges mounted on surface of VKI vane.

Two high sensitivity, fast-response, model XCS-062 Kulite pressure transducers rated to 150 psia were used in the shock tube sections to record absolute pressure. One was located in the driver section of the shock tube and the other was located towards the end of the driven section. The pressure transducer in the driver section gave real time readings so it was known when the desired driver pressure was reached before the diaphragm was broken. The driven section transducer was close to the test section and recorded wave disturbance histories and pressures to help determine wave reflection times and local flow properties. Model PDCR-22 Druck differential pressure transducers rated to 150 psid were used to record static pressures in the test section in the form of two 5-hole arrays in the plexiglass end wall that spanned one pitch length (1.33 in), with one ¼ in upstream and one ¼ in downstream that were centered on the flow path between the instrumented vane and the vane above it in the cascade. Experimental inlet and exit isentropic Mach number were calculated with this data for each run. Total pressure data was taken in one of the probe ports using a pitot tube connected to a short pressure line that in turn was linked to another Druck pressure transducer. Special care was taken in keeping the length of all pressure lines as short as possible to minimize pressure-reading lag; none of the lines were more than about four inches. Heat flux data was sampled at 200 kHz per channel and the pressure data was sampled at 10 kHz. The fully instrumented cascade test section from the heat flux gauge lead wire side is shown in Figure 5. Static pressure leads came out the other side of the test section. In summary, a total of 9 Drucks, 2 Kulites, 1 thermocouple, and 27 (VKI vane) or 28 (LHL vane) platinum thin films were used to obtain the essential data for each run. All the data was processed through a sophisticated high-frequency data acquisition system that allowed easy observation of measurements using MATLAB scripts for each run. Figure 6 shows the basic experimental setup for the shock tube experiment to investigate midspan heat transfer on both the VKI and LHL vane.

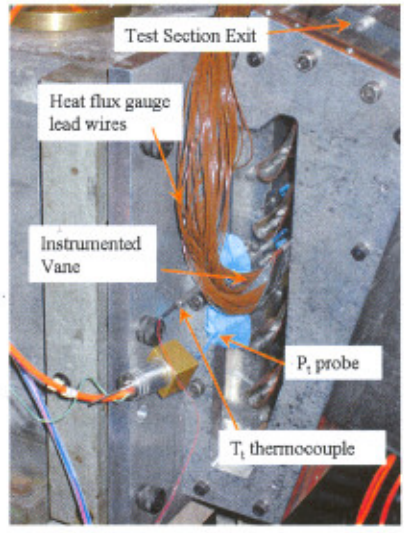

Figure 5 – Instrumented cascade test section positioned at end of shock tube.

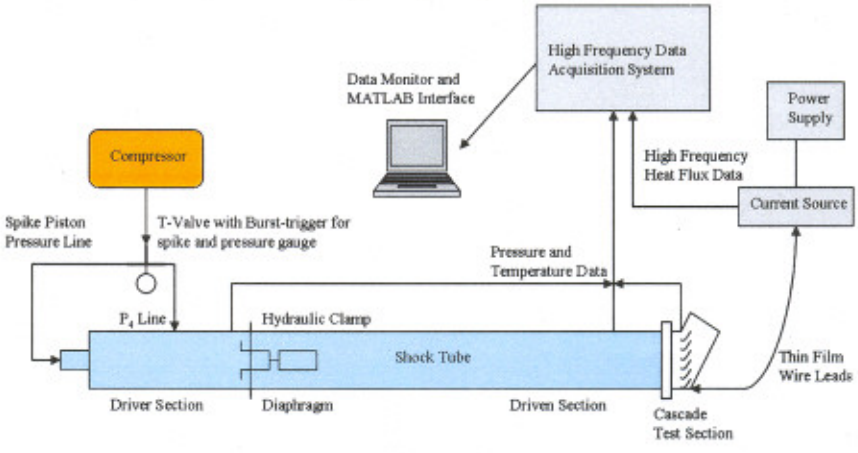

Figure 6 – Shock tube cascade experimental setup.

Uncertainties in the measurement of the midspan heat flux using the platinum thin film gauges is expected to be of order ±10%, as shown in multiple previous studies of heat flux uncertainty using the same instruments[40, 41]. Concerning pressure data error, the Kulite transducer error in the shock tube was ±0.45% of full scale. The Druck transducers used in the test section had uncertainties of approximately ±0.2% of full scale.

IV. Results and Discussion

A. Code Validation Results

Historically, older 2-D heat transfer prediction methods have commonly over-predicted heat transfer rates on both surfaces of an airfoil since non-transitioning turbulence models are used[42]. This agrees with the common industry practice of using a fully turbulent prediction in designing turbine components and cooling systems in order to be conservative with respect to durability. The goal here was to ensure the WILDCAT code gave realistic predictions when compared to data with varying aerodynamic parameters.

Since the pressure loading, or velocity distribution, results from WILDCAT were relied on so heavily for the heat load optimization of the VKI vane, the 2-D pressure loading cases for the VKI data were reviewed. A total of seven experiments were run to analyze the VKI vane at three discrete transonic isentropic exit Mach numbers (M_2). Figures 7a, 7b, and 7c display the VKI experimental results and the numerical prediction for pressure loading plotted against fraction of axial chord by the WILDCAT code for M_2=0.84, M_2=0.875, and M_2=1.02, respectively. Total inlet pressures for the three increasing Mach number runs were 20.8, 21.4, and 23.2 psia, respectively. Also shown to the right of the loadings are local isentropic Mach number plots, showing the acceleration of the flow around the airfoil. The results clearly show that the code predicts the pressure loading profile very well over both the PS and SS of the VKI vane for the range of transonic isentropic exit Mach number. The prediction even fairs well for the obvious supersonic shock regions of the SS for the M_2 = 1.02 case. There is only a very small disparity between the data and the prediction on the SS for lower M_2 runs—probably due to complexities of the SS boundary layer change from a favorable to adverse pressure gradient.

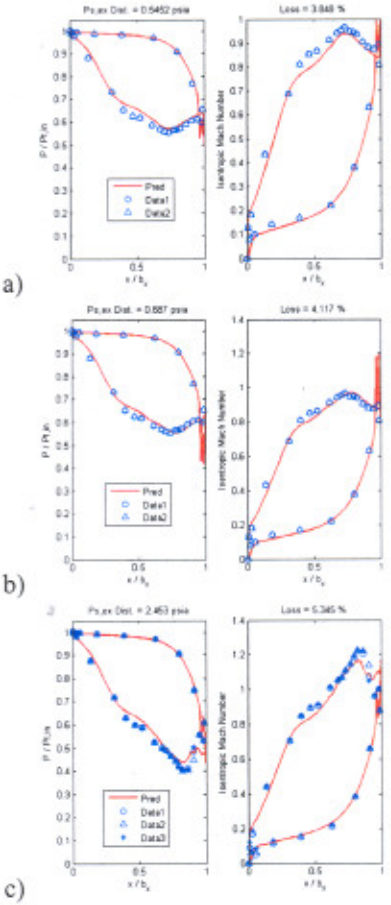

Figure 7 – WILDCAT pressure loading predictions.

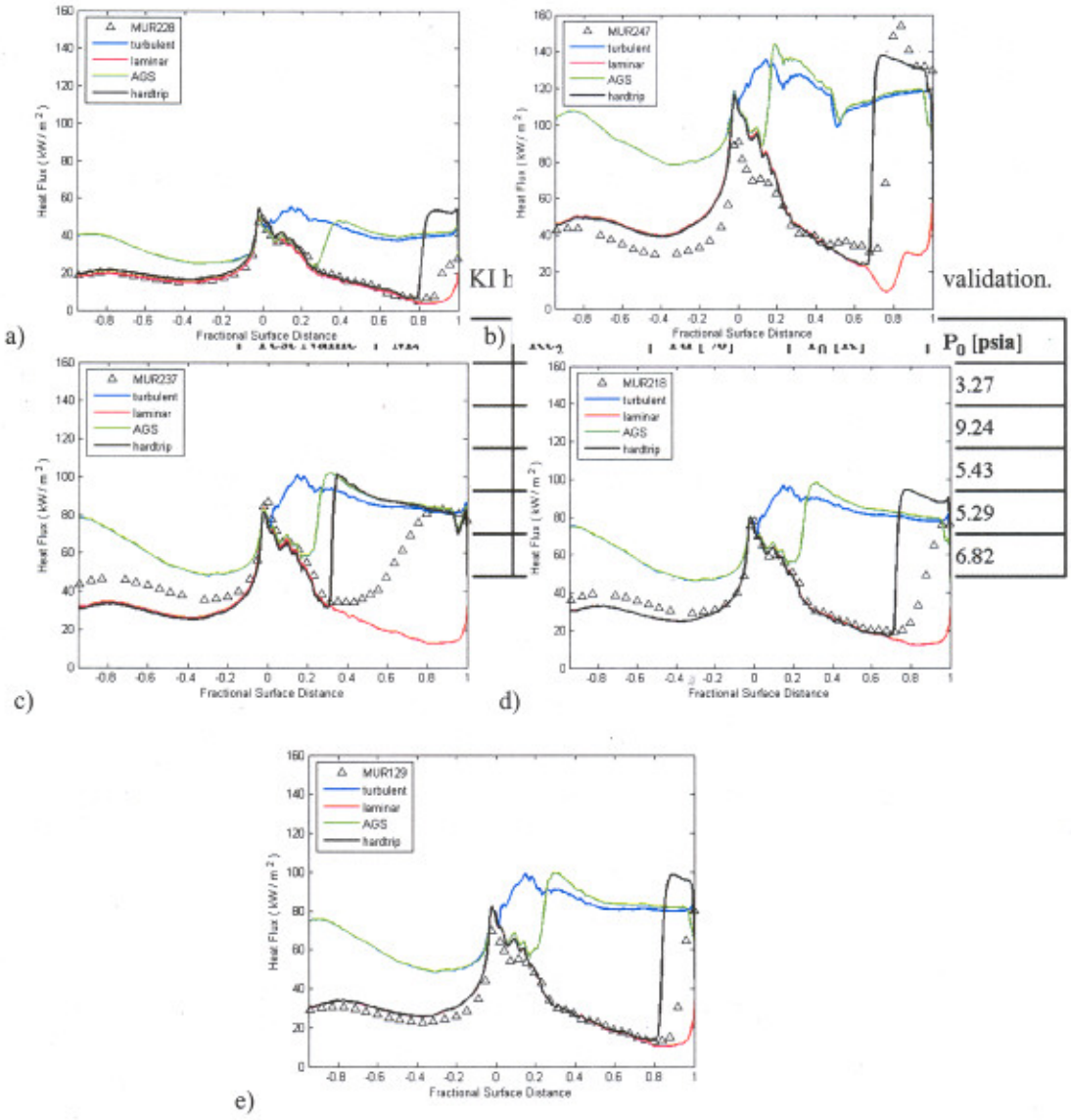

Figure 8 – WILDCAT heat flux surface distribution predictions for varying flow conditions.

The collection of heat transfer runs performed by VKI was narrowed down to five cases for the purpose of comparison of the VKI experimental results and the WILDCAT RANS prediction. The cases selected span a range of three discrete values of exit Reynolds number (Re_2) and turbulence intensity level (Tu) for an approximate M_2 = 0.80, which matches the values to be seen in the cascade shock tube experimental comparison of the VKI and LHL vanes. Table 2 gives the original names of the five runs and their respective key parameters including total temperature and total pressure. The Re values are essentially $5x10^5$, 10^6, and $2x10^6$, while Tu is basically 1%, 4%, and 6%. The exact parameter values shown, except for Re, were entered into the WILDCAT code as flow solver setup parameters to simulate each of these runs with the VKI vane geometry. Figures 8a through 8e show heat flux distributions on the fractional surface distance (PS from -1 to 0, SS from 0 to 1 on the x-axis) of the VKI vane for the VKI data, the WILDCAT laminar viscous prediction, turbulent viscous prediction, the natural Abu-Ghannam and Shaw (AGS) transition model prediction, and a triggered start of transition using the AGS model to compare to VKI data transition onset locations, for the five runs shown in order in Table 2. By entering the fractional surface distance value for which the slope of the line first becomes positive in the VKI data on the SS of the VKI vane, the WILDCAT could perform predictions with a forced transition onset at that point which was termed *hardtrip* in the plots. The hardtrip function caused the laminar viscous equations to be evaluated up until the specified point of transition. In this way a direct comparison of the SS transition could be observed between data and prediction and it

could be shown that by delaying transition, the overall heat load of the vane will decrease since the integral heat flux for the hardtrip is obviously less than for AGS. It can be seen that both transition predictions are somewhat sudden. This is because AGS[31] is only a transition start model in WILDCAT, and not a transition length model, as can be seen in the disparity between the hardtrip AGS line and the VKI data. In addition, the AGS model was derived from experiment solely performed on a flat plate, not on a turbine vane. Some WILDCAT and other open-literature transition models are gleaned from the Narasimha[43] universal intermittency concept, which has been shown to be flawed by Clark et al.[44] In general, the AGS model tends to be more widely used than most models.

Many trends can be seen in the predictions. The predicted vane peak heat load at the leading edge and at the beginning of SS turbulence onset has a strong and relatively proportional Re_2 dependence. SS transition is obviously prevalent even at lower Re runs, so the heat flux predictions provide good motivation for attempting to delay transition to reduce airfoil heat load in the optimization effort. All figures also present a heavy transition onset location dependence on Tu. As Tu increases, transition tends to occur earlier on the SS, which agrees with the work of Blair[13]. This trend was also observed for increasing Re_2. For constant Tu = 1% as Re_2 grew from $5x10^5$ to $2x10^6$, AGS and hardtrip transition onset locations on the SS moved back towards the stagnation point dramatically and the LE peak heat flux nearly tripled. Concerning the natural AGS and turbulent viscous predictions, there appears to be transition to turbulence at about the -0.1 location for all five runs, which accounts for the overprediction of heat transfer on the PS. For the most part, SS laminar predictions are very accurate. On the PS, however, for the high Re case, the laminar boundary layer heat transfer is over-predicted. In contrast, for the high Tu case the PS laminar heat flux is under-predicted, which tends do be in accordance with past studies that have experienced freestream turbulence heat transfer augmentation due to possible secondary or unsteady flow effects[20, 44]. In addition, the laminar viscous prediction only accounts for shear in the boundary layer and has no inherent way to account for unsteady heat and mass transport due to higher levels of Tu. Overall, it appears that for transitional to typical turbine levels of Re_2, the WILDCAT code prediction performs very well, especially for SS characteristics. This contrasts many of the prediction comparisons mentioned earlier in the literature survey[7, 14, 15]. For high Tu, PS laminar heat transfer is under-predicted. For high Re_2, PS laminar heat transfer is over-predicted; however, the SS heat flux is captured well. A reputable 2-D Navier-Stokes code has now been properly validated against a good range of accurately obtained turbine-representative data and the WILDCAT code can be used for a vast variety of turbine component design and optimization tasks.

B. VKI vs. LHL Airfoil

After the lengthy and iterative process previously outlined was executed, the re-design and optimization of the VKI tested vane for the objectives of reduced leading edge heat transfer and delayed suction side transition yielded impressive results, especially considering limited practical history an innovation of this turbine component design technique. A direct comparison of the two vanes is given in this section to cover a wide range of aero-thermodynamic flow characteristics and considerations. The reduced heat transfer airfoil that was chosen as a solution for the reduced heat load design will be referred to as the low-heat-load airfoil, or LHL. Using the methodology and constraints described earlier, a solution was finally found after thousands of optimization iterations and weeks of cumulative computing time.

The new LHL vane is different from the VKI vane in that it has a slightly larger leading edge diameter (LED), resulting in a rounder, more even LE structure which will serve to spread out the LE heat load. The LHL vane also has a thicker mid-chord and slimmer TE section for enhanced flow acceleration. Figure 9 is a first view of the reduced heat transfer optimized solution showing the midspan cross-section airfoil geometry for the LHL vane.

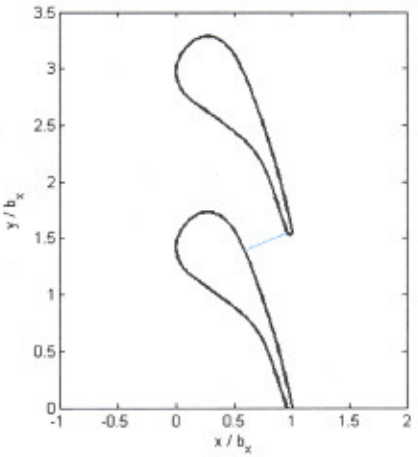

Figure 9 – LHL vane cross-section geometry.

To reiterate, the two main goals of the re-design process were to lower the LE peak heat load and delay the onset of transition on the SS as far as possible by driving the minimum static-to-total pressure ratio, $P/P_{t,in}$, or maximum Mach number, back as far as possible towards the TE. Many different airfoil shapes were observed during the process of the

Table 3 – Final candidate airfoils from optimization process compared to VKI vane.

Airfoil	Minimum SS $P/P_{t,in}$ coordinate $(x/b_x, P_s/P_{t,in})$	Loss (%)	Integral Heat Load (kW/m²)	LE Peak Heat Load (kW/m)
VKI	(0.51, 0.61)	3.521	4.170	112.5
Best hand-iterated	(0.58, 0.65)	3.359	4.265	95.4
GA (987)	(0.70, 0.63)	3.118	4.248	96.0
GA (1508)	(0.75, 0.63)	3.198	4.271	96.1

optimization. After literally weeks of computing time, the results were narrowed down to a healthy group of airfoil geometry candidates. Table 3 compares the properties most relating to the goal of the reduced heat transfer optimization for the original VKI vane, the best airfoil that could be created by hand-iterations (changing parameters by hand and re-running WILDCAT repeatedly), and two good candidates that resulted from the genetic algorithm (GA). The coordinates, x/b_x and $P_s/P_{t,in}$, in the second column are of the point of minimum static-to-inlet-total pressure ratio on the suction side of the vanes. A higher value in x increased the probability of delayed transition wile a lower value in y showed a greater overall acceleration of SS flow in keeping the boundary layer laminar. The GA airfoils given are the 987th and 1,508th optimization iteration that resulted when the two objectives, which were translated into proper fitness functions, were enforced. The values were taken from WILDCAT runs of the midspan geometries using a heat transfer grid at 10,000 iterations and the laminar viscous assumption.

Observing the values in Table 3 it is clear that the GA was very successful in realizing the two main optimization objectives. The 987 and 1508 airfoils had GA fitness scores of 44 and 51, respectively, while the next best airfoil created by the GA had a score of only 30. Naturally, these two stood out and were suitable as a final choice. From here, one airfoil had to be chosen to progress further in the study to be tested experimentally for reduced heat transfer. The aerodynamic losses, integral heat loads and LE peak loads of the two GA airfoil solutions are essentially the same. While the 987 has slightly better numbers for these three categories, it was eliminated in favor of the 1508 airfoil. Knowing the two main objectives of the optimization, the peak loads were the same, and the fact that the 1508 airfoil moved the minimum pressure ratio point towards the TE a whole 5% of the surface distance over the 987 airfoil, this made it the definitive choice. This is a significant design improvement for delaying transition with an x-coordinate of minimum pressure ratio 24% closer to the TE of the wetted suction surface distance compared to the VKI vane. Figures 10a and 10b compares the predicted pressure loadings and heat flux surface distributions of the VKI and LHL vanes by running the WILDCAT code at the design conditions of MUR237 ($Re_2 = 10^6$, $M_2 = 0.8$, and $Tu = 4\%$) with the AGS transition model. As the flow over a turbine nozzle guide vane normally has laminar and turbulent regions with transition in between on both the pressure and suction surfaces for most operating conditions, the focus of the heat transfer comparison stayed with the AGS prediction. The laminar and turbulent prediction comparisons yielded similar trends. The VKI curves are visually much smoother than those of the LHL, but the LHL vane would prove to be a much better performing vane concerning all aspects of turbine vane performance. It can be seen that the LHL vane even has a slightly lower percentage pressure loss. Concerning separation, neither of the vane loading profiles indicate that separation is not an issue for this set of conditions. In addition, the pressure side fluctuations of the LHL vane plot do not ultimately cause transition to turbulence as seen in Figure 10b.

The LHL vane clearly has a much lower leading edge heat load, delayed transition by as much as 20% of the SS distance over VKI, lower integrated heat load, and better aerodynamic qualities with lower loss. Concerning downstream unsteady wakes, the LHL vane also reduced vane exit static pressure ratio distortion 3.3%. It is clear that the larger leading edge of the LHL vane worked well at evening out and lowering the peak heat load at the geometric stagnation point. Instead of spiking like VKI and creating a local hot spot, the heat flux stays low and fluctuates slightly, resulting in a 15% reduction in LE heat load. While the PS heat flux is higher, the SS heat transfer curve behaves stupendously, indicating that the SS curvature was engineered perfectly. These factors all indicate that the computational optimization of the VKI vane to the LHL vane with much more desirable heat

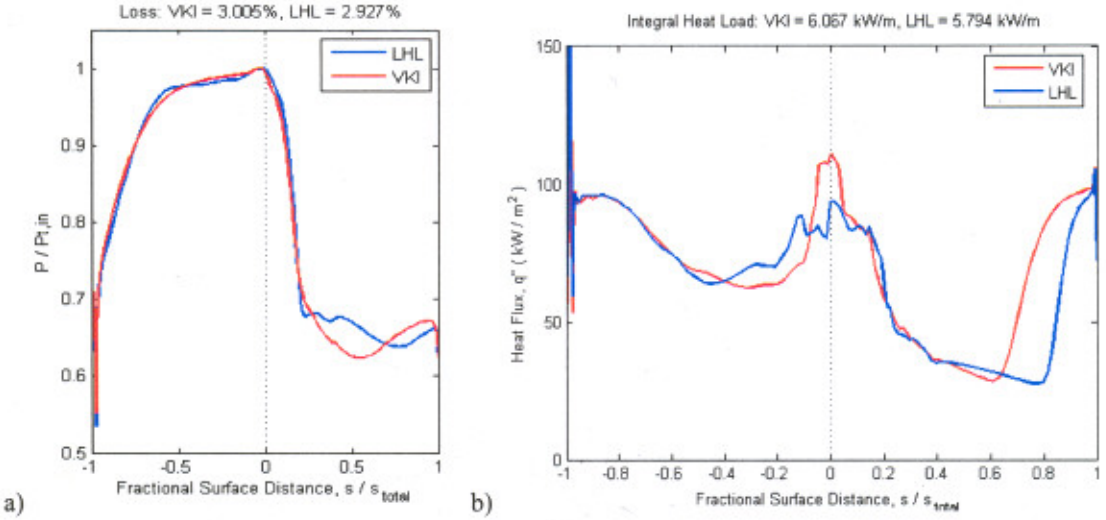

Figure 10 – Pressure loading and heat flux distribution prediction comparisons of the VKI and LHL vanes using the AGS transition model.

transfer qualities was a success. Both of the main re-design and optimization objectives were realized and a worthy candidate has been chosen which can in be tested experimentally to observe if the same heat transfer trends occur in a realistic environment. Finally, because the vanes both choke the inlet flow and perform the same amount of flow turning, the relative performance of the two vanes should remain similar over a range of off-design conditions. This study shows that the SS, and in consequence the integral, heat load could be reduced by delaying transition as a result of moving the minimum SS pressure ratio point back towards the TE as far as possible.

When it comes to the challenge of reduced airfoil surface heat load, and the contenders are VKI versus LHL, LHL wins rather decisively. The study can now progress further and it can be seen how the two might perform in a linear cascade shock-tunnel experiment.

C. Experimental Procedure and Results

Prior to each shock tube run the current source boxes were given time to achieve a steady thermal state. A mylar diaphragm was installed and hydraulically clamped between the shock tube driver and driven sections. A constant current of 4 mA was passed through the gauges. Using a large compressor, the driver section of the tube was pumped to the desired pressure using the real-time read-out of the driver side Kulite transducer. A valve was used to seal off the driver section and another valve was opened to release high pressure air into the line for the spike piston. Ambient temperature and pressure were recorded. Using LabView software, driver pressure could be monitored, and the sampling frequency and data buffer values could be entered along with the desired test time. When the desired driver pressure was reached, the mylar diaphragm was broken sending a normal shock wave propagating down the tube. Data was collected for 2.5 s and written to a MATLAB file for all runs. Observing the raw voltages traces, the average test times were on the order of 5 ms. Figure 11 shows the pitot pressure trace along with Kulite traces and the available test time from which to gather heat flux data. The apparent line thicknesses account for measurement uncertainty. To repeat the process, the old mylar diaphragm was taken out and discarded, the inside of the tube was inspected for shrapnel, and a new diaphragm was installed.

As the tests only used one turbulence grid, the cascade experiments in the shock tube only examined two different values of Tu. The experimental turbulence was measured with a TSI 1210 T1.5 hot-wire probe and an IFA-300 constant temperature anemometer which found grid-in levels of 5 ± 1% and grid-out levels of 2 ± 0.3%. These values include a margin of error as prescribed by Mee and Dickens[45]. Since the thicker diaphragms which could bear more driver pressure (P_4) did not break appropriately in order to create a good moving normal shock, and since lower P_4 runs did not stimulate the thin films enough to create significant changes in raw voltage (thus heat flux), nor are they representative of typical turbine inlet conditions, only a single P_4 of approximately 60 psia was used for all runs. Thus the best four runs of the VKI and LHL vanes with the grid in and out are available for heat transfer analysis. Table 4 gives all run conditions and measured flow properties such as pressures and Mach numbers from the four runs for which heat transfer data will be analyzed. Properties with the subscript "in" are for the test section inlet and properties with the subscript "ex" are for the test section exit ($M_2 = M_{ex}$).

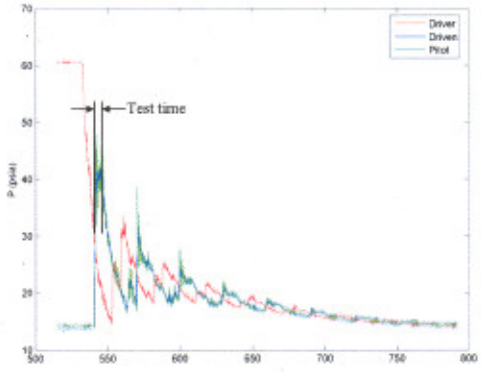

Figure 11 – Pressure histories for a sample shock tube run with test time denoted.

Table 4 – Shock tube experimental run conditions for vane midspan heat transfer measurements.

Run No.	Vane	Grid in?	P_4 (psia)	P_5 (psia)	$P_{t,in}$ (psia)	$P_{s,in}$ (psia)	$P_{s,ex}$ (psia)	P_{amb} (psia)	M_{in}	M_{ex}
10	VKI	Yes	60.23	39.21	39.04	37.79	24.65	14.22	0.216	0.838
11	VKI	No	59.61	40.46	40.36	39.17	25.39	14.22	0.208	0.842
16	LHL	Yes	60.51	40.33	40.12	39.15	25.93	14.16	0.188	0.815
17	LHL	No	59.72	39.38	39.62	38.41	25.51	14.16	0.211	0.819
18	LHL	No	60.39	40.96	41.03	39.86	26.27	14.16	0.203	0.824

All reduced heat transfer data was realized using the methods of Oldfield[47], which is standard for this type of semi-infinite substrate thin film heat flux gauge. MATLAB codes created by Oldfield were used to perform an infinite impulse response (IIR) technique to deboost, filter, and convert raw voltage data to heat flux.

Figure 12a compares midspan heat flux data from run numbers 10 and 11 for the VKI vane with grid in and grid out. It is expected that this plot would show lower heat transfer for a case with no grid relative to a case with the turbulence grid for the same vane, which for the most part is seen, primarily for the high magnitude heat flux characteristics. Near the LE, there appears to be early transition followed by relaminarization. Near the TE, seeing a PS transition to such high heat flux is a surprise knowing the typical historical data in open literature for similar run conditions of M_2 and Re_2. The source of the high heat flux is unknown at this point, or the data is spurious. Both surfaces appear to show rather sudden increase transition to turbulence after passing the LE and an area of extremely high heat transfer relative to the rest of the surface, especially on the SS, which is likely attributable to relaminarization with subsequent transition at about 60% of the fractional distance. The grid out (lower Tu) run appears to transition later with overall lower heat flux magnitudes, which agrees with theory. Gauge 16 on the VKI vane SS turned out to be a dead gauge as seen by its reading of zero heat flux.

Data from the LHL vane grid-in and grid-out runs in Figure 12b show that heat flux is much better-behaved, as compared to the data for the VKI vane, especially on the PS. The distribution is smooth with transition from a laminar boundary layer to a turbulent one at about 30% of the PS, although the entire PS may be laminar. Immediate transition occurs on the SS at about 4% of the SS. Interestingly, each vane experienced early SS transition at the same fraction of surface distance, regardless of the level of Tu. More investigation may be necessary to explain this phenomenon, as historically in numerous experiments, increasing Tu had caused earlier transition onset. The heat transfer from transition to turbulence on the SS is much more pronounced than that of the PS. The experimental SS boundary layer follows theory as the heat transfer is high at first and decreases as the boundary layer grows. The SS heat transfer decreases so much as to suspect relaminarization of the boundary layer, which may be possible as the LHL vane was designed to hold off transition as long as possible. The change in loading in Figure 10a supports this. Again, this second transition event occurs closer to the TE for the grid-out lower Tu case, as it should.

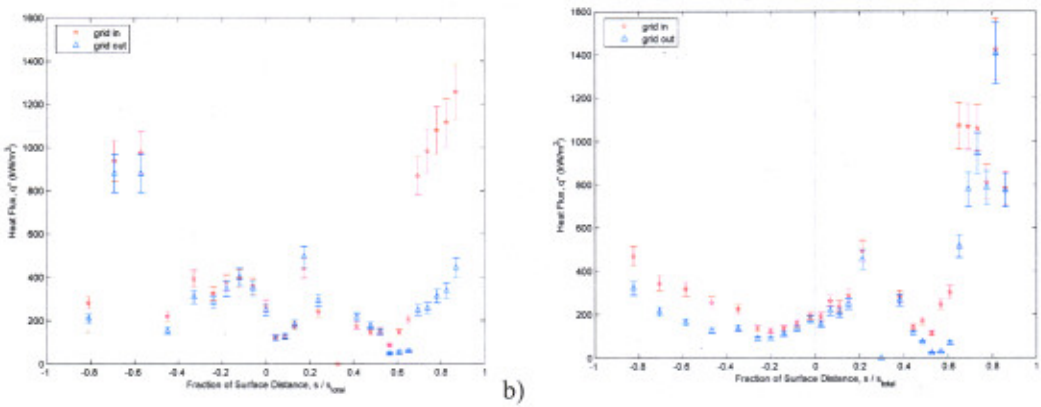

Figure 12 – Grid-in and grid-out heat flux comparisons for the a) VKI and b) LHL vanes.

The heat transfer trends of the VKI and LHL vanes are compared in Figure 13a and 13b. Figure 13a compares shock tube grid-in experimental runs 10 and 16. These are the same data sets shown in Figure 12, just compared differently. The LHL vane clearly exhibits significantly lower PS and lower LE heat transfer by almost 30% of the VKI vane magnitude. This shows that the WILDCAT code successfully predicted that the LHL vane would have lower LE heat transfer relative to VKI. Generally, the LHL vane is mostly laminar, with high heat transfer due to thinned-out boundary layers. Using MATLAB to inspect the data, it turns out that transition occurred at 11% of the SS distance for the LHL vane and 4% for the VKI vane. It appears for the LHL vane the SS there is short-lived laminar boundary layer followed by an immediate transition to turbulence, while the VKI SS appears to rise right up to turbulent levels of heat transfer, slightly lower than that for the LHL vane. This supports the prediction of the LHL vane delaying SS transition (and PS as well) longer than the VKI vane. However, this may not be a significant finding knowing the fact that the levels of heat transfer are so high in the first place—up to 1,600 kW/m^2 for the experimental data compared to only 120 kW/m^2 for the prediction suggests that something currently unexplainable is causing unrealistic heat transfer levels in the shock tube cascade test section. In addition, since both vanes essentially have immediate transition to turbulence, and with the positions of transition onset being so close with this unexplainably augmented heat transfer, it may not be appropriate to compare SS transition with this particular data. A root-mean-square (rms) calculation of the measured PS heat flux in Figure 13a, a technique originally employed

by Owen[47], exaggerated the dominant features in the midspan spatial distribution and showed a 25% delay in PS transition by the LHL vane.

The grid-out cases in Figure 13b for the LHL vane shows more favorable traits than in the case for higher freestream turbulence level. On both surfaces, the LHL has generally lower heat transfer, with an apparent reduction in LE heat flux of over 30% compared to the VKI vane, which is a larger reduction than the design plots which exhibited a 15% reduction. The only exception is the heat transfer near the TE, which is obviously more pronounced on the LHL vane SS. The reason for this occurrence may suggest more experimental investigation is necessary. However, the pressure loading plots and predicted heat transfer for both vanes at these conditions gave no indication of shocks that would originate so far back from the TE, so again it may be more likely that there is relaminarization followed by transition to higher levels of heat transfer.

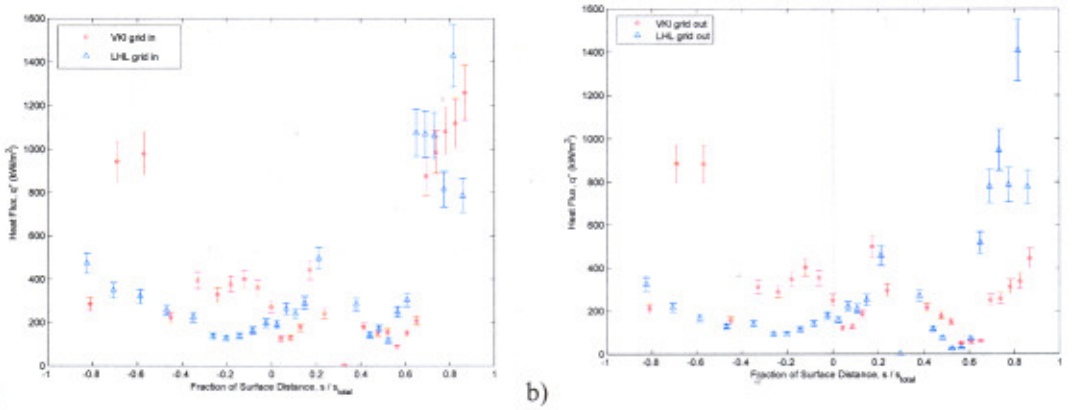

Figure 13 – Direct comparison of VKI and LHL vane midspan heat flux for a) Tu=5% and b) Tu=2%.

Table 5 – Summary of experimental heat transfer characteristics for the VKI and LHL vanes.

Vane geometry	Approximate Tu (%)	LE Heat Flux (kW/m2)	SS transition onset (% SS)	2nd transition location (% SS)	PS transition onset (%)
VKI	2.0	270.93	4	57	45
VKI	5.0	250.33	4	57	10
LHL	2.0	194.21	11	53	None
LHL	5.0	173.87	11	53	35

The shock tube proved to be an inexpensive and highly repeatable rig for examining heat transfer on the VKI and LHL vanes to find that the LHL vane exhibited generally lower heat flux, especially at the leading edge. One of the two goals that were established for obtaining a heat load optimized vane was met when it came to the experimental data. An additional benefit may be seen in the lower PS heat flux due to delayed transition due to the loading. Table 5 is given to review the experimental heat transfer attributes pertaining to the LE and SS transition of the vanes. In summary, a vane that was successfully optimized computationally for reduced heat transfer has fared rather well in an initial experimental study with inlet flow conditions similar to a turbine.

D. Comparison of Heat Transfer Data to WILDCAT Prediction

A final investigation of experimental heat flux was conducted by comparing the data with WILDCAT predictions for the same conditions of the grid-in shock tube runs, since the magnitude of heat flux was so high. As so many predictions of heat transfer data in open literature in the past have disregarded heat flux in favor of predicting Stanton number, it is desirable to meet the challenge of predicting heat flux directly since it is the primary driver for turbine engine cooling flow requirements[42]. Figure 14 gives the laminar and turbulent WILDCAT predictions for the high Tu cases for each vane. The WILDCAT boundary conditions included the effect of increased initial enthalpy as seen in Ref 41. For both vanes, LE heat flux is predicted very well, and as the flow gets

closer to the TE, the prediction becomes less accurate. Overall, the turbulent prediction tends to be closer to the data on both vane surfaces, but even the fully turbulent simulation under-predicts the measurement. This primary trend of under-prediction of data demands further investigation. Presuming that the predictions are closer to what the vanes would experience in a steady, more turbine-representative environment than the shock-tunnel, a range of possible phenomena could account for the heat transfer augmentation in the experiments. Such gross under-prediction of experimental data is not entirely uncommon in open literature concerning similar vane and blade heat transfer studies[8, 12, 14, 15, 16, 20]. For example, consider the work of Finke et al.[48] The authors compared multiple 2-D and 3-D Navier-Stokes and multi-stage Euler codes to midspan heat transfer data from a low aspect ratio turbine vane cascade test section obtained in the CALSPAN reflected-shock tunnel (See Ref 14). The augmented heat transfer relative to the code predictions was at the time attributed to vane surface roughness. However, it seems doubtful that the surface roughness of rig-quality hardware would result in heat transfer augmentation of turbulent flow by as much as 50% on both the PS and SS of the vane. There is a plethora of pertinent data collected in the CALSPAN shock tunnel, but there are few instances of accurate prediction of turbine vane heat transfer as compared to the measurements. Thus, it is postulated that test time of the AFRL shock tunnel (which is substantially smaller than that obtained in the CALSPAN facility) is not long enough to create an appropriate flow-field to take turbine-representative heat transfer measurements.

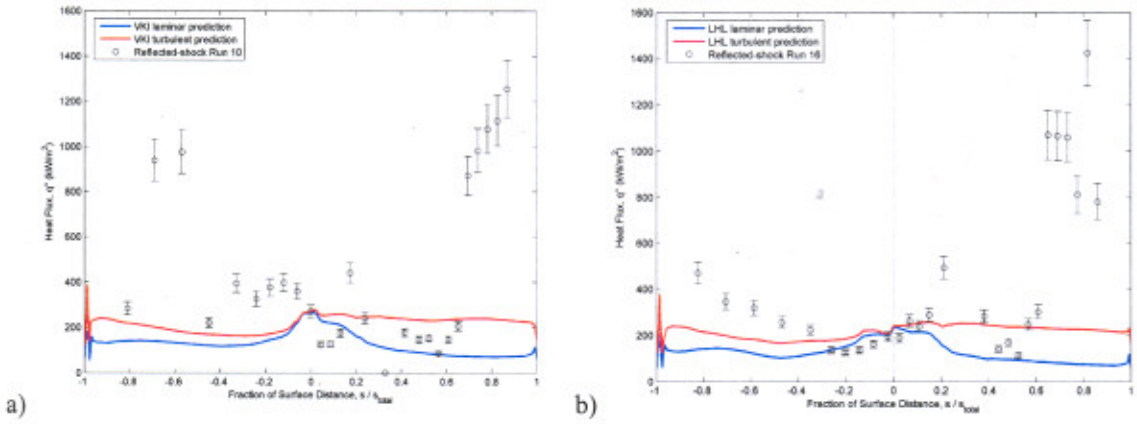

Figure 14 – Grid-in WILDCAT predictions of experimental heat flux for a) VKI and b) LHL vanes.

The time it takes a particle to pass through the test section under steady state conditions can be calculated from the conditions seen in the test section for the VKI and LHL cascade experiment. Analyzing a WILDCAT prediction gives this particle transit time to be about 0.75 ms for the vane design conditions of MUR237. The pressure field, otherwise known as the potential flow-field, sets up on a time-scale that is significantly less than the particle transit time since finite pressure waves propagate at the local flow speed plus the local sonic speed. For this example, a finite pressure wave would propagate through the test section in about 0.2 ms. Hence, flow in the test section is set up sufficiently for assessment of inlet total and inlet- and exit static pressures at about 1 ms after flow start. This is one reason why there has been little difficulty historically in predicting pressure loadings using computational methods and comparing the results to reflected shock data. However, viscous disturbances are well known to propagate at a fraction of the local flow speed, so consequently, over the same time scale, boundary layers are significantly less developed relative to the potential flow field. One would not expect this in a longer run time facility such as the isentropic light piston tube (ILPT) used by Oldfield et al.[37] or facilities with even longer run times such as the AFRL TRF (on order of 3 s). Thus, boundary layers formed over the surfaces of VKI and LHL vanes in the reflected shock tunnel test section in the current experiment may be significantly underdeveloped and thinner than that seen over a longer run time. This means exceptionally high levels of heat transfer (and shear stress), which was observed in the experimental data of this study. This explains the accurate prediction of LE heat transfer with the prediction becoming worse farther downstream towards the TE. According to the premise above, at any given time, the boundary layer nearer the LE on either surface would be more developed than the boundary layer nearer the TE of the vane.

The suggestion outlined above may have implications in the real world today concerning future propulsion technology. While the unsteadiness resulting from the shock tube has fundamentally repetitive, decreasing amplitude waves due to ambient pressure equalization, other more high-tech devices provide consistent, high amplitude, high velocity, unsteady wave phenomena. It has been suggested to use pulse-detonation combustors

instead of steady flow (i.e. deflagration) combustion turbine engines due to the increased thrust-specific fuel consumption. Following the lessons learned in these experiments, one can surmise that at full operating conditions a pulse-detonation combustor positioned upstream of a conventional turbine may cause a periodic variation in boundary layer thickness on the turbine inlet vanes. This in turn may result in significantly increased heat transfer relative to levels seen in conventional motors, which themselves are life limited. Successful design of a pulse detonation combustor with an integrated turbine may be critically dependent upon keeping heat flux magnitudes under control. In addition, remember that in this experiment, no valve was required to achieve the reflected shock conditions. It is unlikely that detonation waves would be swallowed by a downstream vane row, which by definition presents a decreasing area to the wave. The inlet vane annulus and multiple turbine stages would act as obstructions to the pulse detonation combustor, and multiple shock reflections would occur inside as a result.

As a final point, the capability of prediction of the heat transfer in the 2-D linear vane cascade in shock-tunnel flow has proven to be better than expected for the elevated heat transfer levels of the experiments, especially for leading edge heat transfer. The priority of this effort was to show that a validated code could be used to optimize a vane geometry that has lower heat load qualities relative to the nominal design. Both the code and the experiments have shown that the heat-load optimized LHL vane exhibits lower heat transfer distributions in general compared to the VKI vane, with both design objectives having been met. From here, it is plausible that the WILDCAT code could be used in a variety of further turbine design and optimization projects including the reduction of turbine nozzle guide vane heat transfer.

V. Conclusions

A number of significant findings were made as a result of this complete study concerning both numerical prediction and experimental assessment of turbine component heat transfer. The WILDCAT Reynolds-Averaged Navier-Stokes flow solver was validated over a wide range of turbine inlet conditions (Re_2, M_2, and Tu) giving accurate predictions of vane midspan heat transfer and pressure loading against an extensive database of light piston compression tube facility experiments at the von Karman Institute. The now validated WILDCAT code in union with the AFRL turbine design and analysis system (TDAAS) was used (with two types of optimization algorithms) to generate an optimized turbine nozzle guide vane midspan geometry (LHL vane). The design successfully reduced leading edge peak heat transfer by 15% and delayed suction side transition 24% closer to the trailing edge compared to the nominal VKI vane. In addition, for the Abu-Ghannam and Shaw transition model, the LHL vane showed lower integral heat load as well as lower loss, suggesting that the optimized vane had more desirable aerodynamic qualities as well. Reflected shock short duration tests in a linear cascade experiment allowed turbine-inlet experimental comparisons of the VKI and LHL vanes with and without a turbulence grid installed at similarity conditions consistent with a turbine inlet. Transient, spatially resolved, unsteady heat flux was measured at midspan. The Low Heat Load (LHL) vane exhibited LE heat transfer levels 28% lower than the VKI vane for estimated freestream turbulence of 5% and 31% lower for freestream turbulence of 2%. The LHL vane delayed PS transition 25% relative to the VKI vane. However, early transition, followed by relaminarization was experienced on the SS of the vanes. However, subsequent transition to turbulence near the trailing edge caused any conclusions as to whether the LHL vane significantly delayed transition on the suction side to be too ambiguous at this time.

Further investigation of heat transfer due to unsteady wave phenomena is called for as excessive heat flux levels for both vanes were measured near the TE. It was postulated that the short duration experimental runs (5 ms) of the shock tube were inadequate for the viscous flow field to establish itself. So, the boundary layers that formed on the vane surfaces were correspondingly thinner, and this caused higher than expected heat flux measurements. Nevertheless, there was undoubtedly a decrease in relative heat transfer for the LHL vane compared to the VKI vane. Lastly, a further attempt to validate the WILDCAT code was made by comparing laminar viscous and turbulent viscous predictions to the experimental heat flux data collected using the shock tube. Leading edge heat flux was well-predicted, but a significant under-prediction of the data was experienced for most of the pressure and suction surfaces of both the VKI and LHL vane geometries. Again, this was consistent with thin, underdeveloped boundary layers. This is to be expected since the experimental heat transfer (at least towards the TE of the vanes) was for the most part unsteady while the WILDCAT prediction was a steady flow prediction.

Acknowledgments

The authors would like to acknowledge the contributions of R. J. Anthony, M. Ooten, and J. Dagg for their technical support on this effort. Additional support from individuals from the Air Force Research Laboratory and the Air Force Institute of Technology are also greatly appreciated.

References

[1] Johnson, Jamie J. Optimization of a Low Heat Load Turbine Nozzle Guide Vane. Masters Thesis. School of Engineering, Air Force Institute of Technology (AU), Wright-Patterson AFB OH. March 2006.

[2] Nicholson, J.H, Forest, A. E., Oldfield, M. L. G., and Schultz, D. L. "Heat Transfer Optimized Turbine Rotor Blades—An Experimental Study Using Transient Techniques", *ASME Journal of Engineering for Gas Turbines and Power*, Vol. 106, January 1984, pp. 173-182.

[3] Elrod W. C., Gochenaur, J. E., Hitchcock, J. E., and Rivir R. B., "Investigation of Transient Technique for Turbine Vane Heat Transfer Using A Shock Tube," International Gas Turbine Symposium, September 1985.

[4] Fillingim, Patrick K. *Flat Plate and Turbine Vane Cascade Heat Transfe Investigation Using A Shock Tube*. Masters Thesis. School of Engineering, Air Force Institute of Technology (AU), Wright-Patterson AFB OH. December 1985.

[5] Dunn, M. G. and Stoddard F. J., "Studies of Heat Transfer to Gas Turbine Components", Calspan Corporation, Buffalo, New York, 1977, pp. 1-48.

[6] Dunn, M. G. and Hause, A., "Measurement of Heat Flux and Pressure in a Turbine Stage", *ASME Journal of Engineering for Power*, Vol. 104, January 1982, pp. 215-223.

[7] Wistanley, D. K., Booth, T. C., Dunn, M. G., "The Predictability of Turbine Vane Convection Heat Transfer", AIAA Paper No. 81-1435.

[8] Consigny, H. and Richards, B. E., "Short Duration Measurements of Heat-Transfer Rate to a Gas Turbine Rotor Blade", *ASME Journal of Engineering for Power*, Vol 104, July 1982, pp. 542-551.

[9] Simoneau, R. J. and Simon, F. F., "Progress towards understanding and predicting heat transfer in the turbine gas path", International Journal of Heat and Fluid Flow, Vol. 14, No. 2, June 1993, pp. 106-128.

[10] Dunn, M. G., Rae, W. J., and Holt, J. L., "Measurement and Analysis of Heat Flux Data in a Turbine Stage: Part I – Description of Experimental Apparatus and Data Analysis", *ASME Journal of Engineering for Gas Turbines and Power*, Vol. 106, January 1984, pp. 229-233.

[11] Dunn, M. G., Rae, W. J., and Holt, J. L., "Measurement and Analysis of Heat Flux Data in a Turbine Stage: Part II – Discussion of Results and Comparison with Predictions", *ASME Journal of Engineering for Gas Turbines and Power*, Vol. 106, January 1984, pp. 234-240.

[12] Dunn, M. G., "Heat-Flux Measurements for the Rotor of a Full-Stage Turbine: Part I – Time-Averaged Results", *ASME Journal of Turbomachinery*, Vol. 108, July 1986, pp.90-97.

[13] Blair, M. F., "Influence of Free-Stream Turbulence on Boundary Layer Transition in Favorable Pressure Gradients", *ASME Journal of Engineering for Power*, Vol. 104, October 1984, pp. 743-750.

[14] Dunn, M. G., Martin, H. L., and Stanek, M. J., "Heat-Flux and Pressure Measurements and Comparison with Prediction for a Low-Aspect-Ratio Turbine Stage", *ASME Journal of Turbomachinery*, Vol. 108, July 1986, pp. 108-115.

[15] Rae, W. J., Taulbee, K. C., and Dunn, M. G., "Turbine-Stage Heat Transfer: Comparison of Short-Duration Measurements with State of the Art Prediction", AIAA Paper No. 86-1465.

[16] Haldemann, C. W., and Dunn, M. G., "Heat Transfer Measurements and Predictions for the Vane and Blade of a Rotating High-Pressure Turbine Stage", ASME Paper No. GT2003-38726.

[17] Blair, M. F., Dring, R. P., and Joslyn, H. D., "The Effects of Turbulence and Stator/Rotor Interactions on Turbine Heat Transfer: Part II – Effects of Reynolds Number and Incidence", *ASME Journal of Turbomachinery*, Vol. 111, June 1988, pp. 97-103.

[18] Galassi, L., King, P. I., Elrod, W. C., "Effects on Inlet Turbulence Scale on Blade Surface Heat Transfer", AIAA Paper No. 90-2264.

[19] Kays, W. M. and Crawford, M. E., *Convective Heat and Mass Transfer*, McGraw-Hill Book Company, New York, 1993.

[20] Giel, P. W., Van Fossen, G. J., Boyle, R. J., Thurman, D. R., and Civinskas, K. C., "Blade Heat Transfer Measurements and Predictions in a Transonic Turbine Cascade", NASA/TM Paper No. 1999-209296.

[21] Radomsky, R. W., and Thole, K. A., "Detailed Boundary Layer Measurements on a Turbine Stator Vane at Elevated Freestream Turbulence Levels", ASME Paper No. 2001-GT-0169.

[22] Boyle, R. J., Ames, F. E., and Giel, P. W., "Predictions for the effects of Freestream Turbulence on Turbine Blade Heat Transfer", ASME Paper No. GT2004-54332.

[23] Arts, T., Lambert de Rouvroit, L., and Rutherford, A. W., "Aero-Thermal Investigation of a Highly Loaded Transonic Linear Turbine Guide Vane Cascade", von Karman Institute for Fluid Dynamics, September 1990.

[24] Durbin, P., Eaton, J., Laskowski, G., and Vicharelli, A., "Transonic Cascade Measurements to Support Turbulence Modeling", *Air Force Office of Scientific Research, Contractors Meeting in Turbulence and Rotating Flows*, 2004, pp. 57- 62.

[25] Obayashi, S. and Tsukhara, T., "Comparison of Optimization Algorithms for Aerodynamic Shape Design", *AIAA Journal*, Vol. 35, No. 8, August 1997, pp. 1413-1415.

[26] Anguita, D., Cravero, C., Filz, C., Rivieccio, F., "An Innovative Technique for the Aerodynamic Design of Turbine Blade Profiles Using Artificial Intelligence", *Proceedings of the 33rd AIAA Fluid Dynamics Conference*, Orlando, FL, 2003.

[27] Clark, J. P., "An Integrated Design, Analysis, and Optimization System for Turbine Airfoils", AFRL Internal Report, 2004.

[28] Dorney, Daniel. J. and Sondak, Douglas. L. *WILDCAT: Program User's Manual*. April 2001.

[29] Dorney, D. J. and Davis R. L., "Navier-Stokes Analysis of Turbine Blade Heat Transfer and Performance", *ASME Journal of Turbomachinery*, Vol. 114, October 1992, pp. 795-806.

[30] Baldwin, B. S. and Lomax, H., "Thin Layer Approximation and Algebraic Model for Separated Turbulent Flows", AIAA Paper No. 78-257.

[31] Abu-Ghannam, B. J. and Shaw, R., "Natural Transition of Boundary Layers—The Effects of Turbulence Pressure Gradient and Flow History," *Journal of Mechanical Engineering Science*, Vol. 12, No. 5, pp. 1-18, 1980.

[32] Huber, F., personal communication.

[33] Graziani, R. A., Blair, M. F., Taylor, J. R., and Mayle, R. E., "An Experimental Study of Endwall and Airfoil Surface Heat Transfer in a Large Scale Turbine Blade Cascade", *ASME Journal of Engineering for Power*, Vol. 102, pp. 257-267, April 1980.

[34] York, R. E., "Experimental Investigation of Endwall Heat Transfer and Aerodynamics in a Linear Vane Cascade", *ASME Journal of Engineering for Gas Turbines and Power*, Vol. 106, January 1984, pp. 159-167.

[35] Nicholson, J. H., Forest, A. E., Oldfield, M. L. G., Schultz, D. L., "Heat Transfer Optimized Turbine Rotor Blades—An Experimental Study Using Transient Techniques", ASME Journal of Engineering for Gas Turbines and Power, Vol. 106, January 1984, pp. 173-182.

[36] Frye, John W. *Thin-Film Heat Transfer Gages*. Masters Thesis. School of Engineering, Air Force Institute of Technology (AU), Wright-Patterson AFB OH. March 1966.

[37] Gochenaur, John E. *Investigation of Heat Transfer to a Turbine Blade Cascade Using Shock Tube*. Masters Thesis. School of Engineering, Air Force Institute of Technology (AU), Wright-Patterson AFB OH. December 1984.

[38] Anthony, R. J., Jones, T. V., and LaGraff, J. E., 2005, "High Frequency Surface Heat Flux Imaging of Bypass Transition," ASME Journal of Turbomachinery, Vol. 127, pp. 241-250.

[39] Anthony, R. J., Oldfield, M. L. G., Jones, T. V., and LaGraff, J. E., "Development of High Density Arrays of Thin Film Heat Transfer Gauges," *Proceedings of the 5th ASME/JSME Thermal Engineering Joint Conference*, San Diego, CA, 1999. Paper No. AJTE99-1659.

[40] Clark, J. P., Polanka, M. D., Meininger, M., and Praisner, T. J., "Validation of Heat-Flux Predictions on the Outer Air Seal of a Transonic Turbine Blade", *ASME Journal of Turbomachinery*, Vol. 128, July 2006.

[41] Polanka, M. D., Clark, J. P., White, A. L., and Meininger, M., "Turbine Tip and Shroud Heat Transfer and Loading Part B: Comparisons Between Prediction and Experiment Including Unsteady Effects", ASME Paper GT-2003-38916.

[42] Dunn, M. G., "Convective Heat Transfer and Aerodynamics in Axial Flow Turbines", ASME Paper No. 2001-GT-0506.

[43] Narasimha, R., "On the Distribution of Intermittency in the Transition Region of a Boundary Layer", *Readers' Forum, Journal of the Aeronautical Sciences*, pp. 711-712, 1957.

[44] Clark, J. P. and Praisner, T. J., "Predicting Transition in Turbomachinery, Part I – A Review and New Model Development", ASME Paper No. GT2004-54108.

[45] Mee, D. and Dickens, T., "OUEL Blowdown Wind Tunnel Inlet Turbulence Measurement", Internal memorandum, Oxford University, July 1987.

[46] Oldfield, M. L. G., "Guide1 to Impulse Response Heat Transfer Signal Processing, Ver. 2", OUEL Report No. 2233/2000, Oxford, UK, 2000.

[47] Owen, F. K., "Transition Experiments on a Flat Plate at Subsonic and Supersonic Speeds", AIAA Journal, Vol. 8, No. 3, pp. 518-523.
[48] Finke, A. K. and Sharma, O. P., "Low Cost, High-Temperature Blade. Appendix A – Aerodynamic and Heat Transfer Analysis of the Low Aspect Ratio Turbine (LART)", Air Force Research Laboratory Paper No. AFWAL-TR-85-2053.